©2004 by *Economic Geology*
Vol. 99, pp. 789–806

# Formation of a Paleothermal Anomaly and Disseminated Gold Deposits Associated with the Bingham Canyon Porphyry Cu-Au-Mo System, Utah

Charles G. Cunningham,†

*U.S. Geological Survey, 954 National Center, Reston, Virginia 20192*

Gerry W. Austin,

*Kennecott Utah Copper Company, P.O. Box 232, Bingham Canyon, Utah 84006*

Charles W. Naeser,

*U.S. Geological Survey, 926A National Center, Reston, Virginia 20192*

Robert O. Rye,

*U.S. Geological Survey, MS-963, Box 25046, Denver Federal Center, Denver, Colorado 80225*

Geoffrey H. Ballantyne,

*Rio Tinto Technical Services, 5295 South 300 West, Suite 300, Murray, Utah 84107*

Robert G. Stamm,

*U.S. Geological Survey, 926A National Center, Reston, Virginia 20192*

and Charles E. Barker

*U.S. Geological Survey, MS-977, Box 25046, Denver Federal Center, Denver, CO 80225*

## Abstract

The thermal history of the Oquirrh Mountains, Utah, indicates that hydrothermal fluids associated with emplacement of the 37 Ma Bingham Canyon porphyry Cu-Au-Mo deposit extended at least 10 km north of the Bingham pit. An associated paleothermal anomaly enclosed the Barneys Canyon and Melco disseminated gold deposits and several smaller gold deposits between them. Previous studies have shown the Barneys Canyon deposit is near the outer limit of an irregular distal Au-As geochemical halo, about 3 km beyond an intermediate Pb-Zn halo, and 7 km beyond a proximal pyrite halo centered on the Bingham porphyry copper deposit. The Melco deposit also lies near the outer limit of the Au-As halo. Analysis of several geothermometers from samples collected up to 22 km north of the Bingham Canyon porphyry Cu-Au-Mo deposit indicate that most sedimentary rocks of the Oquirrh Mountains, including those at the gold deposits, have not been regionally heated beyond the "oil window" (less than about 150°C). For geologically reasonable heating durations, the maximum sustained temperature at Melco, 6 km north of the Bingham pit, and at Barneys Canyon, 7.5 km north of the pit, was between 100°C and 140°C, as indicated by combinations of conodont color alteration indices of 1.5 to 2, mean random solid bitumen reflectance of about 1.0 percent, lack of annealing of zircon fission tracks, and partial to complete annealing of apatite fission tracks. The pattern of reset apatite fission-track ages indicates that the gold deposits are located approximately on the 120°C isotherm of the 37 Ma paleothermal anomaly assuming a heating duration of about $10^6$ years. The conodont data further constrain the duration of heating to between $5 \times 10^4$ and $10^6$ years at approximately 120°C. The $\delta^{18}O$ of quartzite host rocks generally increases from about 12.6 per mil at the porphyry to about 15.8 per mil approximately 11 km from the Bingham deposit. This change reflects interaction of interstitial clays in the quartzite with circulating meteoric water related to the Bingham Canyon porphyry system. The $\delta^{18}O$ and $\delta^{13}C$ values of limestone vary with respect to degree of recrystallization and proximity to open fractures. Recrystallized limestone at the Melco and Barneys Canyon gold deposits has the highest $\delta^{18}O$ values (about 30‰), whereas limestone adjacent to the porphyry copper deposit has the lowest values (about 10‰). The high $\delta^{18}O$ values for the recrystallized limestone at Barneys Canyon and Melco strongly suggest that mineralization was related to low temperature fluids with exceptionally high $\delta^{18}O_{H_2O}$ values such as could be derived from water in a crater lake of an active volcano.

The age of formation of the gold deposits has been interpreted to range from Jurassic to Eocene. The mineralized rocks at the Barneys Canyon and Melco deposits are likely the same age as the geochemically similar deposits that are present in north-striking, late faults that cut the Bingham Canyon porphyry. The patterns of apatite and zircon fission-track data, conodont color alteration indices, solid bitumen reflectivity, stable isotope

† Corresponding author: e-mail, cunningham@usgs.gov

data, and mineral zoning are consistent with the gold deposits being genetically related to formation of the 37 Ma Bingham porphyry deposit. We interpret the disseminated gold mineralization to be related to collapse of the Bingham Canyon hydrothermal system in which isotopically heavy, oxidizing, acidic waters, possibly from an internally draining acidic crater lake, mixed with and were entrained into reduced gold-bearing meteoric water fluids in the collapsing main-stage hydrothermal system. Most of this fluid mixing and cooling was probably located close to the hydrologic interface between the sedimentary basement rocks and overlying volcanic rocks.

## Introduction

THE BINGHAM CANYON porphyry Cu-Au-Mo deposit near Salt Lake City, Utah, has total production and reserves, including the porphyry, adjacent skarns, base-metal replacement deposits, and alluvial gold, of 27.4 million tonnes (Mt) Cu, 1.3 Mt $MoS_2$, and 1,570 t Au (Krahulec, 1997). North of the porphyry deposit, at distances of 6 and 7.5 km, respectively, are the Melco and Barneys Canyon sedimentary rock-hosted disseminated gold deposits. Several similar, smaller gold deposits are also located near Melco and Barneys Canyon. All are within a concentrically zoned geochemical anomaly around the Bingham deposit described by Babcock et al. (1995) and Gunter and Austin (1997). Melco and Barneys Canyon have similar mineralogy and geochemical signatures and appear in the same type of late, northerly striking structures as other disseminated gold occurrences that are present within the Bingham Canyon porphyry.

Previous studies have shown that large intrusive centers such as the Bingham Canyon porphyry system, when intruded to shallow depths, cause widespread circulation of hot fluids in the adjacent host rocks (Cathles, 1977; Norton, 1978). These fluids may leave a thermal imprint on the host rocks that extends beyond the heat source and associated veins and altered rocks. The record of this paleothermal anomaly can provide information about temperature, composition, age, and even duration of the hydrothermal system. Some studies of paleothermal anomalies have predicted the existence and location of unexposed, mineralized porphyry systems before they were drilled and discovered (Naeser et al., 1980; Cunningham et al., 1987; and Larson et al., 1994). Paleothermal anomalies can be detected in the country rocks surrounding the intrusive centers by resetting of fission-track records in suitable minerals, thermal maturation of organic material, crystallographic changes in phyllosilicate minerals, magnetic changes, and changes in the oxygen and carbon isotopic composition of the rocks (Cunningham and Barton, 1984; Beaty et al., 1990). Numerous stable isotope studies indicate the extent of water rock reaction in host rocks around major intrusions (see summary in Taylor, 1997). The formation and preservation of this record depends upon many factors, such as host rock composition, permeability, depth of erosion, and prior thermal and/or fluid history. Sedimentary rock-hosted gold deposits, such as Carlin-type deposits in Nevada, commonly lack optimal host rocks for recording the thermal history related to gold deposition. The rocks may be too thermally mature, lack appropriate organic materials, or lack suitable minerals for fission-track studies. Carlin-type deposits, in particular, are typically hosted by carbonate rocks that record only isotopic exchange with ore fluids near major structures (Pinckney and Rye, 1972; Rye et al, 1976).

In this study, we address several questions about the possible paleothermal anomaly associated with the Bingham Canyon porphyry system. These questions include the following: (1) How far did the hydrothermal system associated with the Bingham Canyon porphyry extend out into the country rocks? (2) Is a paleothermal anomaly preserved and measurable in the sedimentary strata of the Oquirrh Mountains? (3) Are the disseminated gold deposits in these strata genetically related to the Bingham ore-forming hydrologic system and if so, how and when did they form?

A genetic relationship between the Bingham Canyon porphyry copper deposit and the disseminated gold deposits at Melco and Barneys Canyon had been suggested by Babcock et al. (1995), Ballantyne (1998a, b), and Gunter and Austin (1997), but had not been well established prior to this study. The Melco and Barneys Canyon gold deposits are located about 3 km beyond the outer limits of the base-metal replacement deposits associated with Bingham Canyon but still within the As halo. Therefore, it was considered likely that these deposits might have formed in the thermal halo around the porphyry copper deposit. Both carbonate and quartzite host rocks occur in the Bingham Canyon-Melco-Barneys Canyon corridor. Preliminary conodont and solid bitumen reflectance studies indicated that similar rocks in the Oquirrh Mountains have not been heated beyond the “oil window” (about 150°C; Hunt, 1995), and suggested that sedimentary strata at Melco and Barneys Canyon might retain a record of the distal thermal effects of the Bingham system. The quartzites also contain minor quantities of apatite and zircon suitable for fission-track dating.

## Geologic Setting

The Bingham Canyon porphyry Cu-Au-Mo deposit is related to stocks and dikes that intruded into Pennsylvanian quartzites and limestones, mostly of the Bingham Mine Formation of the Oquirrh Group (Peters et al., 1966; Warnaars et al., 1978; Babcock et al., 1995). To the north of the Bingham deposit are overlying interbedded quartzites and sandstones (Fig. 1) of the Lower Permian Freeman Peak Formation, calcareous sandstones of the Lower Permian Diamond Creek Formation, and cherty, phosphatic dolomite and dolomitic siltstone of the Lower Permian Park City Formation (Babcock et al., 1995; Laes et al., 1997). Scattered throughout the quartzites are thin limestone layers. The Melco deposit is hosted in a highly calcareous unit at the base of the Diamond Creek Formation, and the Barneys Canyon deposit is hosted by a dolomitic unit within the Park City Formation. The sedimentary rocks are deformed by thrusting and folding, and the gold deposits are close to the northerly plunging hinge line of the Copperton anticline (Fig. 1).

### *Bingham Canyon porphyry Cu-Au-Mo deposit*

The Bingham Canyon porphyry Cu-Au-Mo deposit is described in a recent compilation of papers in John and

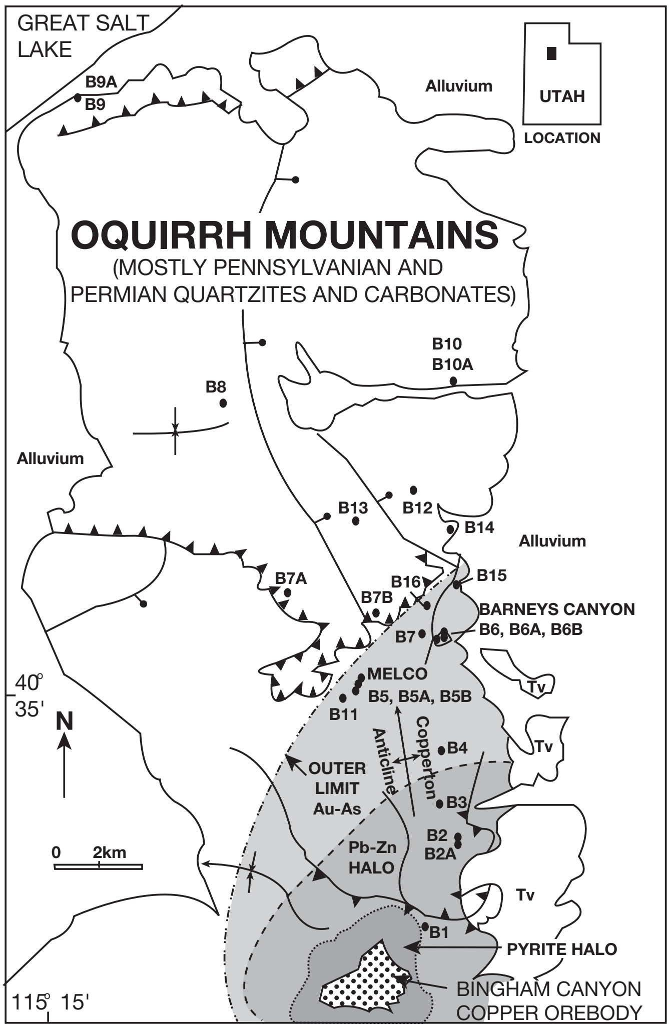


FIG. 1. Simplified map of the northern Oquirrh Mountains, Utah, modified from Babcock et al. (1995) and Laes et al. (1997), showing the location of samples that were collected along a regional traverse. Rocks are mostly Pennsylvanian and Permian quartzite and carbonate rock. Rocks along the east side of the range, denoted by the symbol Tv, are Eocene-Oligocene volcanic-related rocks. Spatial relations between the Bingham Canyon Cu-Au-Mo orebody, pyrite halo, Pb-Zn halo, outer limit of Au-As, and the Melco and Barneys Canyon mines are shown. The Melco mine is about 6 km north of the Bingham Canyon mine.

Ballantyne (1997). Earlier reports include James et al. (1961), Peters et al. (1966), Atkinson and Einaudi (1978), Lanier et al. (1978a,b), Bowman et al. (1987), and Babcock et al. (1995). The deposit and associated intrusions were emplaced during the Eocene. Recent, high-precision age determinations include a U-Pb age of 38.55 ± 0.19 Ma for the earliest intrusion (Parry et al., 2001). Several $^{40}Ar/^{39}Ar$ ages ranging from 40 to 37 Ma are reported for the major igneous rocks and related alteration (Deino and Keith, 1997; Parry et al., 1997, 2001). Mineralization was dated by a composite Re-Os molybdenite age determination of 37.0 ± 0.27 Ma (Chesley and Ruiz, 1997) and an $^{40}Ar/^{39}Ar$ age of 37.1 ± 0.5 Ma from fluid inclusions in mineralized quartz veins (Kendrick et al., 2001).

Calc-alkaline monzonite, quartz monzonite, and quartz latite intrusions of the Bingham intrusive complex are spatially related to the ore. Small volumes of primitive, alkaline intrusions are also present, and Waite et al. (1997) have suggested that they contributed some of the sulfur and metal in the deposit and may have facilitated concentration of volatiles and metals in the upper part of the magma chamber. The Bingham intrusions were emplaced in the deep part of a composite stratovolcano, and approximately 2.5 to 3 km of the volcanic edifice has been removed by erosion (see cross sections in Waite et al., 1997).

The deposit exhibits concentric mineralization and alteration zones that have been well described by Rose (1970), John (1978), and Phillips et al. (1997). In general, an innermost core of relatively barren, potassically altered quartz monzonite porphyry is surrounded by successive shells of molybdenum and copper mineralization in the form of stacked, inverted bowls. Gold distribution generally follows copper (Ballantyne et al., 1997). Phyllically altered rocks are present locally beyond the potassic alteration zone, and skarn deposits are present along the northwest edge of the porphyry copper ore body. A prominent pyrite halo around the copper orebody is overlapped and surrounded by a halo of fissure-controlled Pb-Zn veins that postdate copper mineralization (Rubright and Hart, 1968; Babcock et al., 1995).

*Gold deposits in the Bingham Canyon porphyry district*

Barneys Canyon and Melco contain the largest concentrations of gold in a continuum of geochemically similar veins, smaller economic deposits, subeconomic gold deposits, and gold-in-soil anomalies. The gold mineralization extends 7.5 km north from small bodies of late gold mineralization that cut the porphyry copper mineralization at Bingham Canyon. Three small gold deposits are present within the copper-mineralized zone at Bingham: the Main Hill, Parnell and North ore shoot deposits (Babcock et al., 1995). They contain realgar and orpiment and are mineralogically and geochemically similar to "Carlin-type" disseminated gold deposits (Hofstra et al., 2003). The Main Hill gold mineralization cuts the porphyry copper deposit, the Parnell gold deposit cuts copper-mineralized skarn, and gold mineralization at the North ore shoot occurred at the outer limit of copper-mineralized skarn and locally cuts the skarn (Cameron and Garmoe, 1987; Babcock et al., 1995; Gunter and Austin, 1997). These small deposits occur along late faults on north-trending structures similar to those at Melco and Barneys Canyon.

Gold grades generally are low in most of the pyrite and Pb-Zn halos, but high-grade pyritic gold and arsenic-bearing veins are locally present (Babcock et al., 1995). Three small economic gold deposits occur near Barneys Canyon and Melco, called South BCS, North BCS, and East Barneys, in order of decreasing size. They are located on the axis of the Copperton anticline along northeast-trending structures (Gunter and Austin, 1997). The Southeast Pediment gold prospect, 2.5 km southeast of Barneys Canyon (Gunter and Austin, 1997) is significant because the northern part of the gold occurrence immediately underlies barren but hydrothermally altered 39 Ma volcanic rocks (Deino and Keith, 1997). Gold-associated trace element enrichment extended up into the altered volcanic rocks, but gold mineralization did not

(Gunter and Austin, 1997). On the basis of several thousand soil and rock samples, all of these deposits, occurrences, and prospects lie within a broad Au-As-pyrite anomaly (Fig. 1) that is centered on the Bingham Canyon Cu-Au-Mo deposit and extends to the north along the axis of the Copperton anticline (Babcock et al. 1995; Gunter and Austin, 1997).

*Barneys Canyon gold deposit:* The Barneys Canyon deposit is described in detail by Gunter et al. (1990), Presnell (1992), and Presnell and Parry (1996). It is located 7.5 km north of the north edge of the Bingham pit, about 3 km beyond the outer edge of the Pb-Zn halo, and it is the most distal of the disseminated gold deposits in the area. Mining at Barneys Canyon commenced in 1988 and was completed in 1996 with more than 15 tonnes of gold produced from oxide ore with an average grade of 1.6 g/t Au.

The west wall of the Barneys Canyon pit shows several important relations in the northeast-dipping strata (Fig. 2). The host rocks for gold mainly are cherty dolomite of the Permian Park City Formation. The dolomite, with a prominent phosphatic horizon, is thrust over itself along the Barneys Canyon thrust fault of probable Mesozoic age. Field relations indicate that gold mineralization was younger than thrusting (Gunter, 1992). The economic part of the gold deposit was in the lower-plate rocks near the structurally deformed contact with underlying Diamond Creek sandstones (Austin and Gunter, 1997), but gold mineralization crossed the thrust fault and extended into the upper-plate rocks as well. The mineralized strata are dropped down to the east along the West fault, exposing the older sandstones through a V-shaped window in the wall of the pit (Fig. 2).

The disseminated gold at Barneys Canyon occurs as grains typically less than 2 micrometers across, associated with supergene Fe-oxide pseudomorphs of pyrite and marcasite. As, Sb, Hg, Ba, and Tl are also anomalous in the sedimentary rocks. Mineralization is controlled by high- and low-angle faults and permeable rock units. Alteration consists mostly of decarbonatization of dolomite and calcareous sandstone, argillization of sandstone, and minor silicification (Presnell, 1992; Presnell and Parry, 1992, 1995). Kaolinite and illite coexist in varying proportions, and illite is the predominant clay mineral in the core of the gold deposit (Presnell and Parry, 1992).

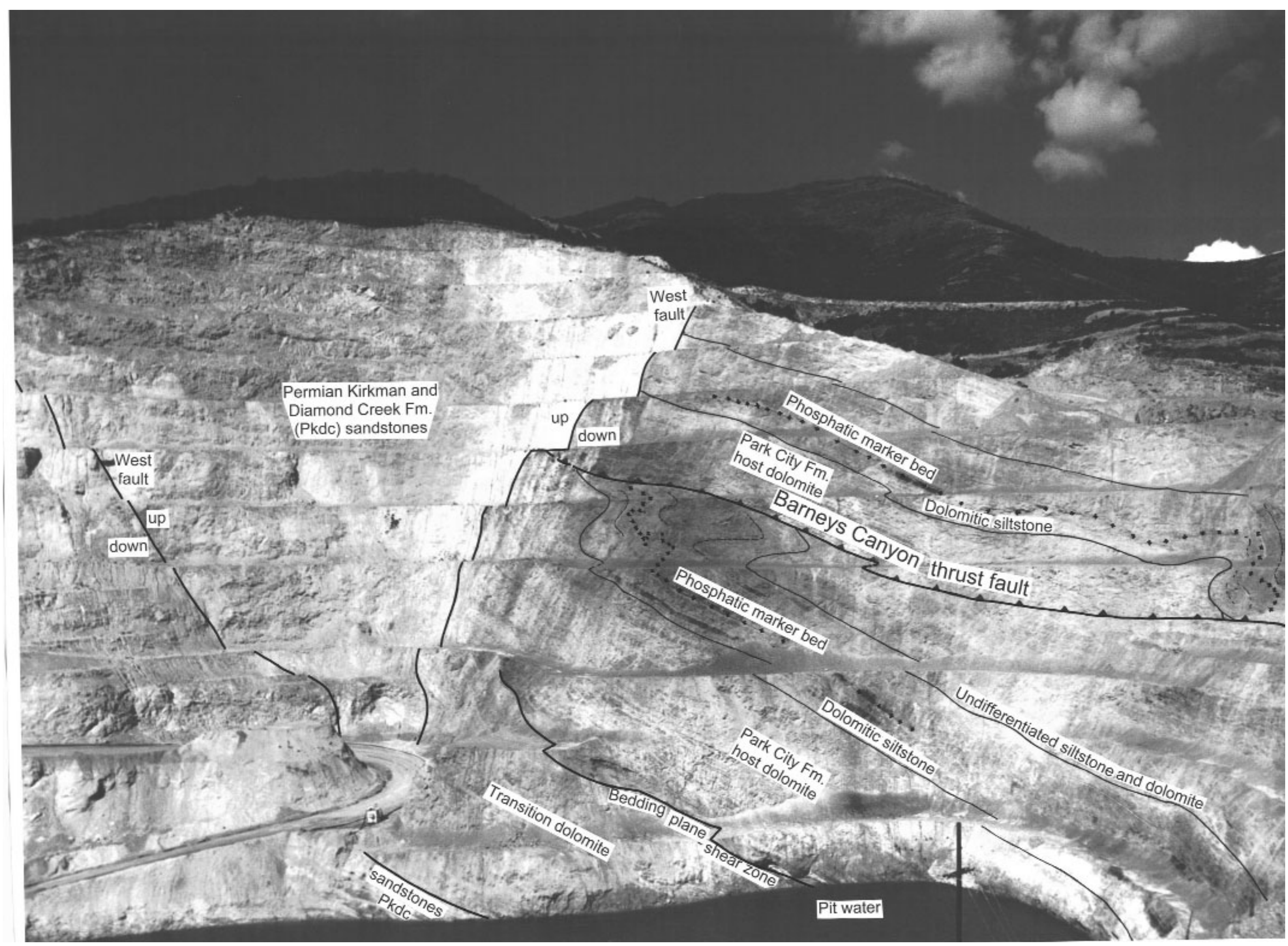


FIG. 2. View of west wall of the Barneys Canyon mine, showing lower Permian Park City Formation carbonate strata in foreground. The Park City Formation contains a thrust fault that is cut by gold mineralization that constrains the maximum age of the deposit. The V-shaped exposure of Permian Diamond Creek sandstone shows through a window in the West fault that down-drops the rocks in the foreground. The Barneys Canyon mine produced more than 15 tonnes of Au.

*Melco gold deposit:* The Melco deposit (Fig. 3) is described in detail by Gunter and Austin (1997) and Austin and Gunter (1997). It is located about 6 km north of the north edge of the Bingham pit (Fig. 1). Melco is similar to Barneys Canyon and contains disseminated gold and anomalous As, Sb, Hg, Tl, and Ba. Mining began in 1989 and was completed in 2001. Melco has proven to be the largest disseminated gold deposit in the district and has produced 37 tonnes of gold produced from both sulfide and oxide ore with an average grade of 2.5 g/t Au. The deposit is structurally controlled and is located on the northwest-dipping limb of the Copperton anticline near an intensely deformed contact between calcareous sandstone and quartzite of the Diamond Creek Formation and quartzite of the Freeman Peak Formation. Gunter and Austin (1977) recognized two episodes of sulfide deposition, the earlier of which is barren and the later of which contains carbon and gold. The paragenetically late gold occurs with pyrite, fine-grained marcasite, and minor arsenopyrite. The gold-mineralized rock is commonly associated with black, carbonaceous material and pods of realgar and orpiment. The mineralized zone follows and is bounded by a set of steeply dipping, diverging N 30 E-striking faults, resulting in an ore zone that widens upwards (Gunter and Austin, 1997). Carbonaceous zones generally follow the same set of faults but locally extend above and laterally beyond the ore zone. Intense supergene oxidation and bleaching is an obvious alteration at Melco, although kaolinite and illite also are present (Gunter and Austin, 1997). There are no known intrusive rocks within 300 m of either Barneys Canyon or Melco. Geological sections suggest that volcanic rocks probably were present within a few hundred meters above the uppermost portions of both deposits prior to erosion.

*Age and origin of the disseminated gold deposits*

The age of the disseminated gold deposits in the vicinity of the Bingham Canyon porphyry Cu-Au-Mo deposit has been controversial because material suitable for dating and demonstrably related to the gold-mineralizing episode has not been found. Presnell and Parry (1996) reasoned that Barneys Canyon was related to a separate hydrothermal system because their observed fluid inclusion temperatures at Barneys Canyon were inconsistent with a reasonable temperature gradient with distance from the Bingham Canyon porphyry Cu-Au-Mo deposit. They dated illites from ore-grade, bedding-plane gouge-like material from Barneys Canyon and obtained slightly discordant Jurassic ages (147 ± 5 Ma and 159 ± 6 Ma; Presnell and Parry, 1992), leading to the proposal that the gold deposit formed during the Jurassic (Presnell and Parry, 1996). Arehart et al. (2003) report U/Th-He dates of 34.9 ± 1.8 Ma from the Bingham Canyon porphyry and 33.1 ±1.6

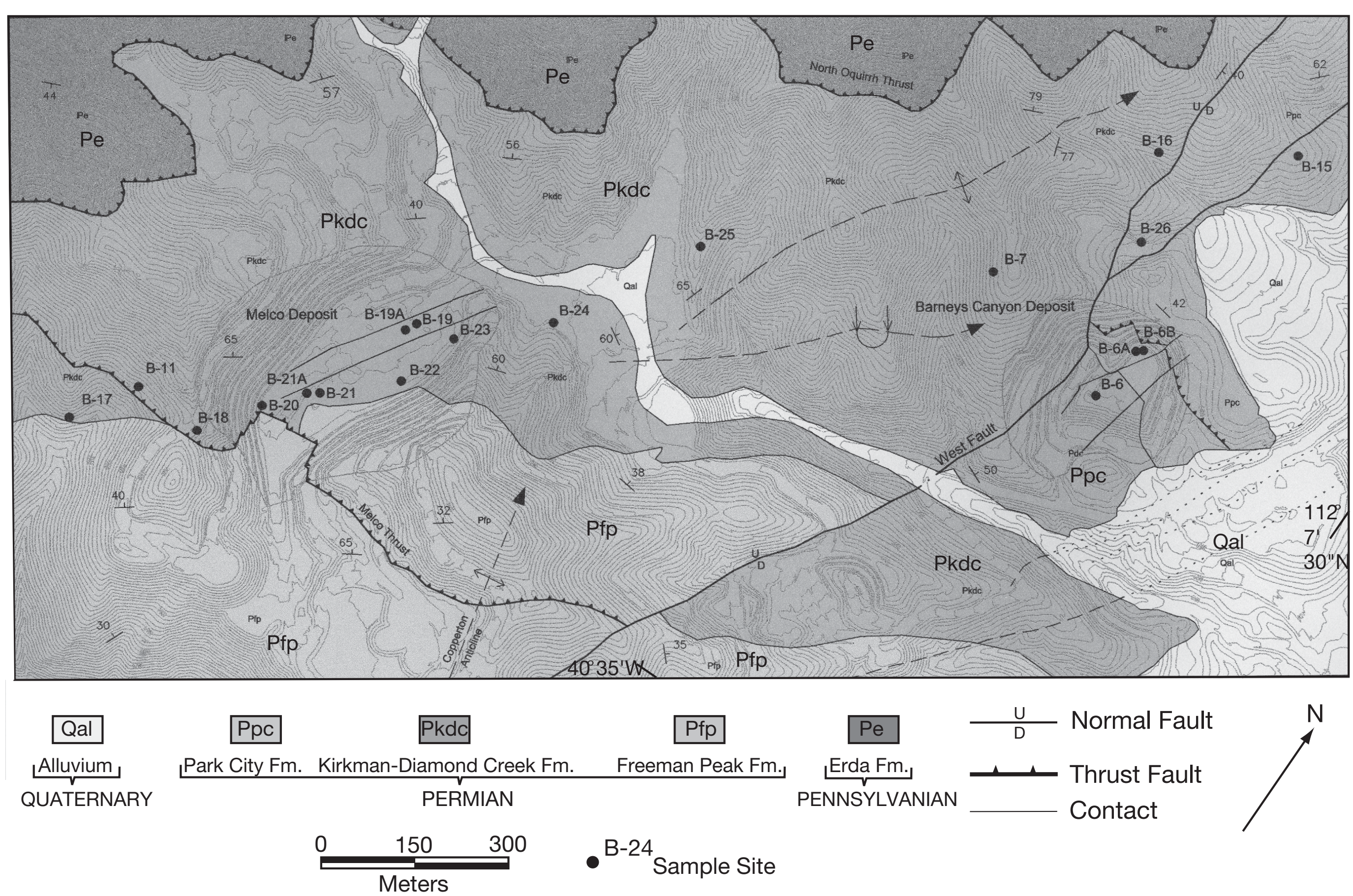


FIG. 3. Geologic map of the Melco and Barneys Canyon gold deposits, Utah, and location of samples along the Melco traverse. Source, files of Kennecott Utah Copper, Bingham Canyon, Utah.

Ma from apatite from Barneys Canyon gold deposit. They interpreted these ages to correspond with cooling of the hydrothermal system below about 75ºC.

The ages of the Barneys Canyon and Melco deposits can be partially constrained by structural relationships. Gold mineralization cuts the Barneys Canyon thrust fault exposed in the pit wall (Fig. 2) and thus is younger than the thrust; however, the age of thrusting is not clear. At least two episodes of eastward- and southeastward-directed thrusting took place in Utah: the Elko orogeny (170–150 Ma: Snoke and Miller, 1988; Thorman et al., 1992) has been documented in northeast Nevada and northwest Utah, and the Sevier orogeny has been documented in the Oquirrh Mountains (110–65 Ma: Armstrong, 1968; Miller, 1990). Presnell (1992) and Presnell and Parry (1995) interpret the Jurassic illite ages to indicate that folding, related thrusting, and mineralization took place in the Late Jurassic (Presnell, 1997). In contrast, Gunter and Austin (1997) and J. Welsh (pers. commun., 2000) believe that the thrusting is early Late Cretaceous and part of the Sevier orogeny. This belief is based, in part, on the correlation of strata between the Oquirrh Mountains and the Center Creek quadrangle, 55 km southeast of Salt Lake City, where recent mapping has demonstrated a Late Cretaceous age for thrusting (Biek et al., 2000). Both gold deposits are structurally controlled by faults related to the Copperton anticline; Melco is on the western hinge zone along a north-northeast–striking fault, whereas Barneys Canyon is present on the northern flank along north– to north-northeast–trending faults (Presnell and Parry, 1996; Presnell, 1997). The Main Hill fault zone within the Bingham Canyon deposit has a similar trend and similar chemistry, and it was apparently active at the same time as the faults that localize gold at Barneys Canyon and Melco.

Babcock et al. (1995) noted a possible genetic relationship between the porphyry deposit and the gold deposits based upon the presence of similar trace element suites at Melco and Barneys Canyon and the late gold mineralization in the Main Hill area of the Bingham mine. Gunter and Austin (1997) noted that Barneys Canyon gold mineralization cuts Sevier age thrusting (ca. 110–65 Ma), that high-grade gold mineralization with a "Carlin-type" trace element assemblage cuts main stage porphyry Cu-Au mineralization, that gold mineralized rock occurs immediately beneath barren but hydrothermally altered volcanic rocks dated at 38.0 ± 0.1 Ma (Deino and Keith, 1997; Hofstra et al., 1999), and that the gold deposits lie within an As-Au halo around the porphyry. All of these observations support the idea that the gold deposits formed at the same time as the intrusions in the Oquirrh Mountains, between 39 and 31 Ma.

The Barneys Canyon and Melco gold deposits exhibit some features of both "Carlin type" (Model 26a of Cox and Singer, 1986) and "distal disseminated Ag-Au type" sedimentary rock-hosted disseminated gold deposits (Model 19c of Cox and Singer, 1990, 1992; Peters et al., 2004). In both types, gold is submicrometer size, disseminated, and associated with As-rich pyrite and marcasite (Hofstra and Cline, 2000). Both types also are present in a wide variety of variably decalcified, silicified, and argillized host rocks. Carlin-type gold deposits are generally larger and have higher grades than distal disseminated Ag-Au deposits, and they characteristically contain stibnite, realgar, orpiment, cinnabar, and Tl sulfide minerals in addition to As-rich pyrite and marcasite (Peters et al., 2004). Another common characteristic of Carlin-type gold deposits is the abundance of black, sooty carbonaceous material that is believed to be relict petroleum (Armstrong et al., 1997, 1998). Carlin-type gold deposits tend to form at depths >2 km, at temperatures of 150º to 250ºC, and from low salinity (<6 wt % NaCl equiv) fluids (Hofstra and Cline, 2000). Distal disseminated Ag-Au deposits are characterized by relatively high Ag and base metal contents. They form at higher temperatures and from higher-salinity ore fluids, possibly with a magmatic component. They contain microscopically visible gold, exhibit K metasomatism, and have a clear spatial and genetic relationship to porphyry systems, in contrast to Carlin-type deposits (Hofstra and Cline, 2000; Theodore, 2000; Peters et al., 2004).

## Materials, Methods, and Data

A suite of representative rock samples was collected on a 22-km traverse from the north edge of the Bingham pit to the north end of the Oquirrh Mountains and from a second traverse across the Melco deposit. The sample locations, formation names, and rock types are listed in Table 1 and are shown on Figure 1. Samples were taken from mine workings and outcrops near the crest of the north-trending Copperton anticline, which predates mineralization. Samples B5, B5A, and B5B are from the Melco mine; B6, B6A, B6B, and B6C are from the Barneys Canyon mine. The quartzite and sandstone units contain about 5 to 10 percent material other than quartz, including zircon, apatite, and local matrix feldspar that generally is altered to clay minerals. A few samples were also collected from limestone, dolomite, and shaley layers (Table 1).

Apatite and zircon were separated by heavy liquids and magnetic separator and then were hand-picked for fission-track studies; these results are presented in Table 2 and Figures 4 and 5. Procedures for fission-track dating and interpretation of annealing effects are described in Naeser (1979). Fission tracks are zones of disruption in a mineral's crystal lattice produced by the passage of massive charged particles, usually owing to the radioactive decay of uranium that was deposited during growth of the crystal. The number of fission tracks produced is a function of the amount of uranium present and time. The tracks can be etched and counted, the amount of uranium measured, and an "age" calculated. The fission-track age is calculated by the zeta method (Hurford and Green, 1983). The zeta method involves dating apatite and zircon from rocks of known age in order to establish the calibration parameters needed to calculate a fission-track age. Once a zeta factor has been determined three measurements are required for calculating the fission-track age of an unknown mineral: the fossil track density ($\rho_s$), the induced track density ($\rho_i$), and a measurement of the neutron dose that the sample received in the reactor ($\rho_d$). The fossil track density is a measurement of the number of tracks that accumulated, from the spontaneous fission of $^{238}U$, since the last time the mineral cooled below the temperature for total track annealing. The induced track density is a measurement of the amount of uranium present in the crystal. The induced tracks are caused by the neutron induced fission of $^{235}U$ in the

TABLE 1. Sample Location, Stratigraphic Unit, and Rock Type of Analyzed Samples from the Oquirrh Mountains, Utah

| Sample | Formation | Rock | Lat 40° N (min) | Lat 40° N (s) | Long 112° W (min) | Long 112° W (s) | Distance (km) | Elevation (ft) | Elevation (m) |
|---|---|---|---|---|---|---|---|---|---|
| B1 | Markham | Quartzite | 32 | 15 | 8 | 30 | 0.71 | 6,680 | 2,036 |
| B1A | Markham | Dolomite | 32 | 15 | 8 | 28 | 0.74 | 6,680 | 2,036 |
| B2 | Curry Peak | Quartzite | 33 | 5 | 7 | 37 | 3.02 | 6,560 | 1,999 |
| B2A | Curry Peak | Quartzite | 33 | 6 | 7 | 34 | 3.1 | 6,560 | 1,999 |
| B3 | Curry Peak | Quartzite | 33 | 35 | 7 | 53 | 3.65 | 5,840 | 1,780 |
| B4 | Freeman | Quartzite | 34 | 24 | 8 | 19 | 4.96 | 7,420 | 2,262 |
| B5 | Diamond | Quartzite | 35 | 6 | 9 | 27 | 6.22 | 7,080 | 2,158 |
| B5A | Diamond | Dolomite | 35 | 3 | 9 | 29 | 6.12 | 7,000 | 2,134 |
| B5B | Diamond | Shale | 34 | 58 | 9 | 30 | 6 | 6,980 | 2,128 |
| B6 | Diamond | Quartzite | 35 | 44 | 8 | 6 | 7.42 | 6,160 | 1,878 |
| B6A | Park City | Dolomite | 35 | 53 | 8 | 7 | 7.7 | 6,160 | 1,878 |
| B6B | Park City | Phosp ss | 35 | 53 | 8 | 1 | 7.72 | 6,160 | 1,878 |
| B6C | Park City | Shale | 35 | 51 | 8 | 3 | 7.64 | 6,160 | 1,878 |
| B7 | Diamond | Quartzite | 35 | 52 | 8 | 22 | 7.6 | 6,820 | 2,079 |
| B7A | Lake Point | Limestone | 36 | 20 | 10 | 39 | 8.82 | 8,560 | 2,609 |
| B7B | Erda | Dolomite | 36 | 4 | 9 | 14 | 8 | 7,440 | 2,268 |
| B8 | Kessler | Quartzite | 38 | 49 | 11 | 41 | 13.66 | 7,960 | 2,426 |
| B9 | Erda | Quartzite | 42 | 43 | 14 | 15 | 21.62 | 4,440 | 1,353 |
| B9A | Erda | Limestone | 42 | 43 | 14 | 11 | 21.6 | 4,440 | 1,353 |
| B10 | Park City | Dolomite | 39 | 3 | 7 | 52 | 13.61 | 5,240 | 1,597 |
| B10A | Park City | Phosp ss | 39 | 3 | 7 | 50 | 13.62 | 5,240 | 1,597 |
| B11 | Diamond | Limestone | 34 | 57 | 9 | 43 | 6 | 7,320 | 2,231 |
| B12 | Diamond | Quartzite | 37 | 45 | 8 | 32 | 11.34 | 6,370 | 1,942 |
| B13 | Diamond | Quartzite | 37 | 33 | 9 | 27 | 11.14 | 6,650 | 2,027 |
| B14 | Park City | Limestone | 37 | 12 | 7 | 46 | 10.28 | 6,220 | 1,896 |
| B15 | Park City | Limestone | 36 | 20 | 7 | 59 | 8.62 | 6,620 | 2,018 |
| B16 | Diamond | Quartzite | 35 | 52 | 8 | 17 | 8.24 | 6,680 | 2,036 |
| B26 | Park City | Limestone | 36 | 3 | 8 | 12 | 7.66 | 6,600 | 2,012 |

Distance is measured from north rim of Bingham porphyry pit

Samples B5, B5A, B5B from Melco; B6, B6A, B6B, and B6C from Barneys Canyon

Curry Peak = Lower Permian Curry Peak Formation (Oquirrh Group), Diamond = Lower Permian Diamond Creek Formation, Erda = Pennsylvanian Erda Formation (Oquirrh Group), Freeman = Lower Permian Freeman Peak Formation (Oquirrh Group), Markham = Markham Member of Pennsylvanian Bingham Mine Formation (Oquirrh Group), Kessler = Pennsylvanian Kessler Canyon Formation (Oquirrh Group), Lake Point = Pennsylvanian Lake Point Limestone (Oquirrh Group), Park City = Permian Park City Formation, Phosp ss = phosphate sandstone

TABLE 2. Fission-Track Ages from the Oquirrh Mountains, Utah

| Sample | Mineral | Number of grains | [1]$\rho_s$ x $10^6$ t/cm$^2$ | [2]Fossil tracks counted | [3]$\rho_i$ x $10^6$ t/cm$^2$ | [4]Induced tracks counted | $X^2$ | [5]$\rho_d$ x $10^4$ t/cm$^2$ | [6]Dosimeter tracks counted | [7]Age Ma ± 2$\sigma$ |
|---|---|---|---|---|---|---|---|---|---|---|
| B-2 | Apatite | 2 | 0.235 | 10 | 3.3 | 70 | P | 3.51 | 2,986 | 27±18 |
| B-3 | Apatite | 10 | 0.953 | 103 | 8.84 | 478 | P | 3.51 | 2,986 | 40 ± 9 |
| B-5 | Apatite | 9 | 0.863 | 115 | 8.2 | 546 | P | 3.51 | 2,986 | 40 ± 8 |
| B-6 | Apatite | 10 | 0.783 | 127 | 3.97 | 322 | P | 3.51 | 2,986 | 74 ± 16 |
| B-1 | Zircon | 10 | 16.1 | 2,307 | 8.04 | 574 | F | 47.5 | 3,464 | 297 ± 41 |
| B-2 | Zircon | 9 | 15.5 | 1,801 | 4.42 | 256 | F | 47.5 | 3,464 | 485 ± 98 |
| B-3 | Zircon | 6 | 22.1 | 682 | 8.42 | 130 | P | 47.5 | 3,464 | 386 ± 75 |
| B-4 | Zircon | 10 | 17.3 | 2,472 | 6.13 | 438 | F | 47.5 | 3,464 | 432 ± 85 |
| B-5 | Zircon | 9 | 15.7 | 2,490 | 5.43 | 430 | F | 47.5 | 3,464 | 425 ± 83 |
| B-6 | Zircon | 10 | 19.2 | 3,034 | 6.38 | 505 | F | 47.5 | 3,464 | 424 ± 125 |
| B-7 | Zircon | 10 | 14.3 | 3,634 | 5.01 | 638 | F | 47.5 | 3,464 | 430 ± 74 |
| B-8 | Zircon | 10 | 17.6 | 2,862 | 7.38 | 598 | F | 47.5 | 3,464 | 393 ± 87 |
| B-9 | Zircon | 10 | 10.3 | 937 | 5.53 | 251 | P | 47.5 | 3,464 | 277 ± 40 |

$X^2$ = Chi square test pass (P) ≥5 percent or fail (F) <5 percent

Insufficient apatite was recovered from these samples to permit both age and track-length analysis

[1] Spontaneous fission-track density

[2] Number of spontaneous fission tracks counted

[3] Induced fission-track density from neutron induced fission of $^{235}U$

[4] Number of induced fission tracks counted

[5] Induced fission-track density in neutron dosimeter

[6] Number of fission tracks counted in determining $\rho_d$

[7] Central age used if sample fails chi square test (Galbraith, 1981;Green et al., 1989), otherwise pooled age used; age calculated using the following zeta calibration values: 10752 (apatite external detector method, SRM 963), 319.6 (zircon external detector method, SRM 962)

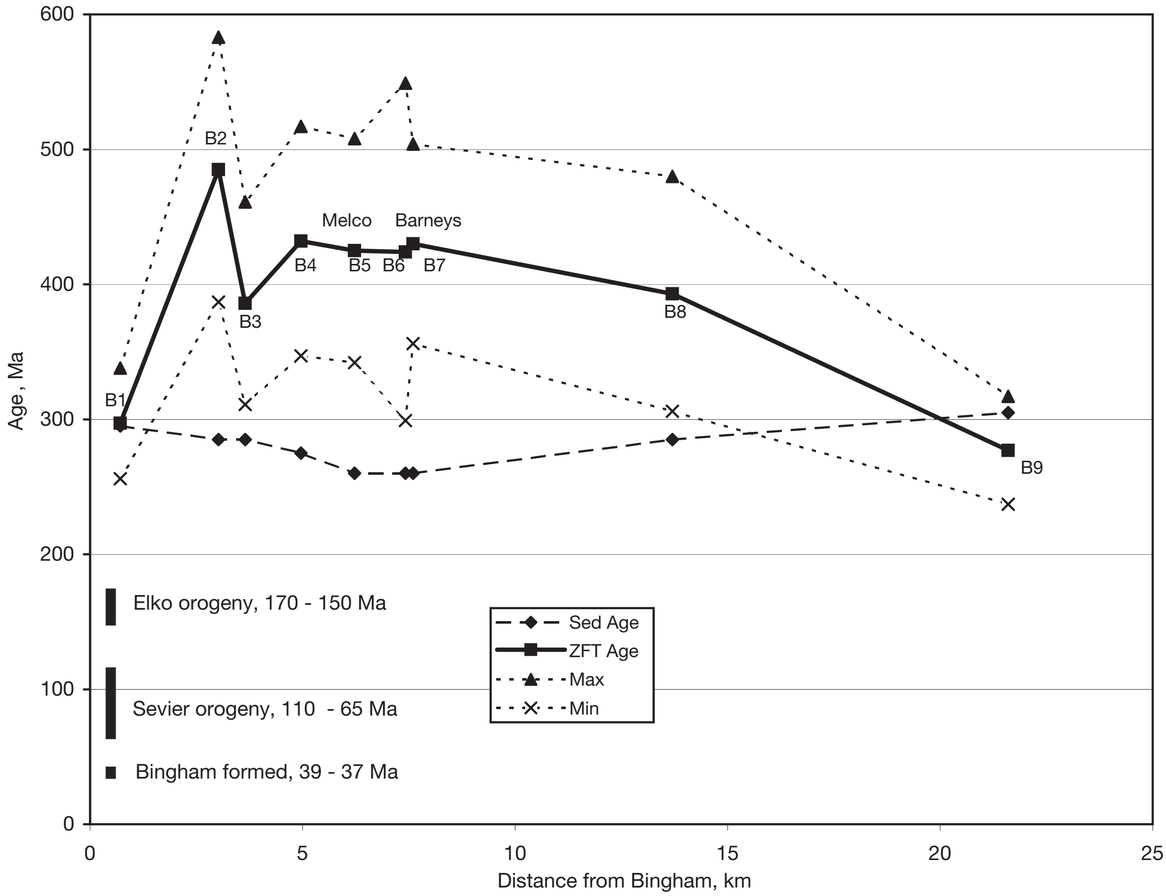


FIG. 4. Fission-track age of zircon (ZFT Age; solid line) versus distance north from the Bingham pit (Table 2). Also shown are 2$\sigma$ error curves and the sedimentation age (Sed Age) of the host formations.

mineral. In order to calculate an age it is also necessary to know the number of neutrons that passed through the mineral during irradiation. This number is determined by counting the number of tracks present in a piece of muscovite that covered a standard glass during the irradiation. The error of a fission-track age is determined from the number of tracks that were counted in determining the respective track densities.

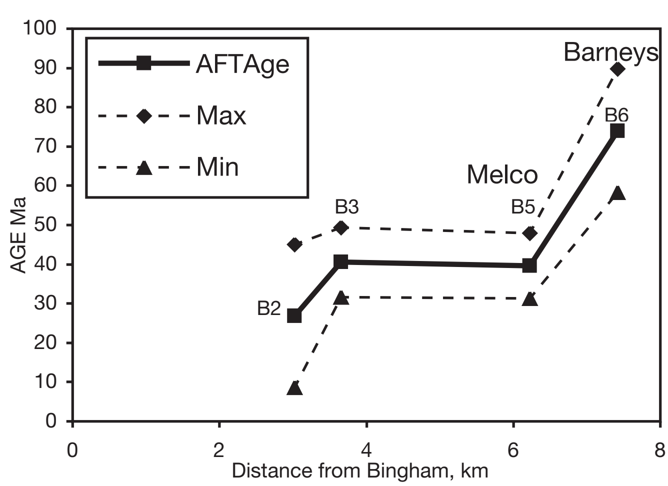


FIG. 5. Fission-track age of apatite (AFT Age; solid line) versus distance north from the Bingham pit (Table 2). Also shown are 2$\sigma$ error curves.

Fission tracks will also anneal if heated. Then the calculated age reflects the postcrystallization thermal history of the mineral (Naeser, 1979). In Figures 4 and 5, the measured age of the mineral, as a function of the distance north from the Bingham Canyon pit, is shown by a solid line. The two-sigma error, which gives the maximum and minimum ages, is shown by the dotted lines above and below the measured age. Figure 3 also shows the age of sedimentation with a dashed line, and for reference, the ages of the Elko orogeny (170–150 Ma), the Sevier orogeny (110–65 Ma), and formation of the Bingham Canyon porphyry deposit (39–37 Ma), discussed further on.

Carbonate rocks were dissolved to remove conodonts to determine their stratigraphic age and thermal history. These data are presented in Table 3. Conodonts change color when heated and the Color Alteration Index (CAI) is a measure of the maximum sustained temperature to which the conodont has been subjected. Procedures and interpretation details are described in Epstein et al. (1977), Harris et al. (1980), and Rejebian et al. (1987). Figure 6 is a time-temperature plot constructed from experimental CAI data, and it is used

TABLE 3. Conodont Data from the Oquirrh Mountains, Utah

| Sample | Stratigraphic age | Fragments | CAI | Temperature (°C) |
|---|---|---|---|---|
| B5A | Late Pennsylvanian | 11 | 2 | 60–140 |
| B6A | Early Permian | 96 | 1.5 | 50–90 |
| B7A | Late Mississippian | 23 | 2 | 60–140 |
| B7B | Middle Pennsylvanian | 84 | 2 | 60–140 |
| B9A | Middle Pennsylvanian | 8 | 5.5–7 | 330–720 |
| B10 | Permian | 2 | 4 | 190–300 |
| B11 | Early Permian | 307 | 2 | 60–140 |
| B14 | Middle Permian | 6 | 2 | 60–140 |
| B15 | Early Permian | 19 | 2 | 60–140 |
| B26 | Early Permian | 30 | 2 | 60–140 |

See Epstein et al. (1977), Harris et al. (1980), and Rejebian et al. (1987) for methodology

CAI = conodont color alteration index

together with data from Barneys Canyon to interpret the thermal history.

Vitrinite and bitumen were examined in polished section and the mean random reflectivity (Ro, in percent) was measured. These data are reported in Table 4. Vitrinite is a coal maceral, commonly woody material, whose reflectance increases when it is heated (Barker and Bone, 1995). Bitumen is condensed, residual petroleum material that congeals, hardens, and also increases its reflectance when heated. Vitrinite and bitumen react irreversibly to temperature increases with a loss of volatiles and are sensitive indicators of the maximum temperature attained. Although vitrinite or bitumen was detected in six samples, only sample B5A from Melco provided enough good material to obtain a statistically valid maximum temperature (Barker and Pawlewicz, 1993, 1994). The technique is limited by the presence of inertinite (a relatively inert high-carbon coal maceral), which may be inadvertently measured instead of vitrinite in sparsely populated high-temperature samples.

Whole-rock oxygen and carbon isotopes were analyzed using standard methods, and the results are given in Table 5. Whole-rock $\delta^{18}O$ as a function of distance from the north end of the Bingham Canyon pit is plotted for quartzite in Figure 7 and for carbonate rocks in Figure 8A. Corresponding whole-rock $\delta^{13}C$ data for carbonate rock are shown in Figure 8B, and $\delta^{13}C$ versus $\delta^{18}O$ data for carbonate rocks are plotted in Figure 9. Detailed sampling of the quartzite adjacent to the Melco deposit was also carried out at approximately the same stratigraphic level as the orebody (Fig. 3). The samples were analyzed for Au, a trace element suite, and $\delta^{18}O$. These results are given in Table 6 and shown in Figure 10.

## Thermal Data

All methods used in this study to constrain paleotemperatures around Bingham Canyon deposit are functions of both time and temperature. Similar fission track, CAI, and bitumen data can result from heating at a high temperature for a short period of time or at a low temperature for a long period of time. But the different materials (conodonts, apatite, zircon, vitrinite, bitumen) react to increasing temperature at different rates. Thus the temperatures reported are "integrated" temperatures, and time must be considered as well. Another factor to consider is channeled flow—when brief pulses of small quantities of hot fluid rapidly pass along a major structure of a deposit without greatly heating the wall rocks. The disseminated nature of the ore and altered rocks at Barneys Canyon and Melco argue for generally pervasive flow, but possible indications of channeled flow may be seen in fluid inclusion, stable isotope, and trace element data, discussed below.

### *Fission track indicators*

Fission track annealing rates for apatite and zircon have been investigated by Naeser (1979, 1981). At 160°C, apatite fission tracks will begin to anneal in less than 1,000 years. Apatite will anneal all of its tracks in 1 h at 350°C, in 1,000 years at about 180°C, and in 1 m.y. at about 135°C. Fission-track annealing in zircon takes place at temperatures between about 210° and 270°C (Hurford, 1986; Brandon et al., 1998) for heating times less than 1 m.y.. At temperatures above this range tracks are not stable and are annealed almost as fast as they form.

TABLE 4. Estimated Maximum Temperature of Vitrinite and Solid Bitumen on the Basis of Geothermometers of Barker and Pawlewicz (1994) and Barker and Bone (1995)

| Sample | Rock | Organic matter | Mean Ro (%) | Standard deviation (%) | Sample size | Maximum temperature (°C) | Comments |
|---|---|---|---|---|---|---|---|
| B1A | Black dolomite | Solid bitumen | 2.64 | 0.43 | 5 | 180 | Dark dolomite |
| B2 | Quartzite | Barren | | | | | |
| B2A | Sandstone | Solid bitumen | 1.28 | | 1 | | Dark sandstone |
| B5 | Quartzite | Barren | | | | | Melco mine |
| B5A | Dolomite | Solid bitumen | 0.95 | 0.16 | 27 | 100 | Melco mine; reliable data |
| B5B | Black shale | Solid bitumen | 1.19 | 0.08 | 2 | | Melco mine |
| B6B | Sandstone | Barren | | | | | Barneys Canyon mine |
| B6C | Black shale | Vitrinite | 2.69 | 0.56 | 5 | 220 | Barneys Canyon mine |
| B7A | Limestone | Barren | | | | | |
| B7B | Dolomite | Barren | | | | | |
| B9A | Limestone | Solid bitumen | 1.91 | 0.41 | 6 | 140 | |
| B10 | Dolomite | Barren | | | | | |
| B10A | Phosp ss | Barren | | | | | |
| B11 | Limestone | Barren | | | | | |

Ro % = mean random reflectivity

Sample size = number of fragments measured

TABLE 5. Whole-Rock Stable Isotope Data from a Regional Traverse

| | | $\delta^{18}O$ (‰) | | | |
|---|---|---|---|---|---|
| Sample | Rock | Quartzite | Limestone | $\delta^{13}C$ | Comments |
| B1 | Quartzite | 12.6 | | | |
| B1A | Dolomite | | 10.3 | –1.4 | Dark rock |
| B2 | Quartzite | 13 | | | |
| B3 | Quartzite | 14.1 | | | |
| B4 | Quartzite | 14.2 | | | |
| B5 | Quartzite | 12.6 | | | Melco mine |
| B5A | Dolomite | | 29.8 | 0.9 | Melco mine |
| B6 | Quartzite | 14.4 | | | Barneys Canyon mine |
| B6A | Dolomite | | 28.5 | 0.7 | Barneys Canyon mine |
| B7 | Quartzite | 12.5 | | | |
| B7A | Limestone | | 22.7 | –0.4 | |
| B7B | Dolomite | | 26.3 | –0.3 | |
| B8 | Quartzite | 15 | | | |
| B9 | Quartzite | 18.6 | | | |
| B9A | Limestone | | 19.9 | –0.1 | |
| B10 | Dolomite | | 23.8 | –0.6 | |
| B11 | Limestone | | 20.6 | –2.6 | |
| B12 | Quartzite | 14.4 | | | |
| B13 | Quartzite | 15.8 | | | |
| B14 | Limestone | | 24.4 | –1.8 | 7.5 km N BC |
| B15 | Limestone | | 13.8 | 0.6 | 2.5 km N BC |
| B16 | Quartzite | 13.8 | | | |
| B26 | Limestone | | 25.2 | –1.4 | 1 km N BC |

N BC = North of Barneys Canyon mine

Zircon fission tracks in samples B2-B8 (Table 2, Fig. 4) give ages that are older than the ages of sedimentation and have not been reset, thus they record the provenance ages of the zircon. Zircon fission track ages have large $2\sigma$ errors reflecting the large variation in the ages of individual zircons (Fig.4); for example, the large error of ±125 Ma from sample B6 was due to a single zircon that gave an age of 1.2 Ga, reflecting the inhomogeneity of the different source rocks.

The closure temperature for retaining fission tracks in zircon is estimated to be between 225° and 250°C (Hurford, 1986; Brandon et al., 1998). These temperatures are derived from geologic and laboratory studies of fission-track fading (annealing) in zircon. The zircon data alone constrain the maximum temperature of the rocks since deposition to about 225° to 250°C (Hurford, 1986; Brandon et al., 1998). No indication of heating is present in the central section of the Oquirrh Mountains either by a Jurassic event or during Sevier thrusting. However, sample B9, at the north edge of the Oquirrh Mountains (Table 2 and Fig. 1) shows the effects of postdepositional heating, including the lowering of the apparent zircon fission-track age to less than the stratigraphic age, the lessening of the error range, and CAIs of 5.5 to 7 (Fig. 4, Tables 2 and 3). These data may indicate that heating took place during thrusting of the Permian rocks against the abutment of the Precambrian rocks of Antelope Island, located a few km north of sample B9, or the presence of a concealed intrusion. At the south end of the traverse, zircon from sample B1 (Table 4), less than 1 km from the Bingham pit, shows the effects of partial annealing of zircons owing to heating above 225°C in the thermal aureole of the Bingham deposit. The thermal aureole from 3 km (Sample B2) to beyond 7.5 km (Sample B6, Barneys Canyon) did not reach temperatures of more than 225°C, because zircons are not significantly annealed.

Apatite data (Table 2 and Fig. 5) show that apatite fission tracks are completely annealed and give the age of the Bingham Canyon porphyry copper deposit all the way out to Melco at 6 km. The apatite fission tracks are partly annealed at Barneys Canyon (7.5 km) to give an age intermediate between the age of the Bingham Canyon porphyry copper deposit and the age of the unheated apatite in the central part of the Oquirrh Mountains.

*Conodont indicators*

Conodonts give CAI values that range from 1.5 to 7 (Table 3). The CAIs of about 2 (Table 3) throughout much of the Oquirrh Mountains further constrain the time and temperature history of the regional host rocks to a maximum temperature of 140°C. There are several areas that CAIs indicate were locally heated, which provides insight into variations in the thermal history of the host rocks.

A statistically reliable CAI of 1.5 (Table 3, sample B6A) at Barneys Canyon indicates that the maximum sustainable temperature was about 90°C. Corresponding data for Melco (Table 3, sample B5A) gives a CAI of 2, which corresponds with a maximum sustainable temperature of 140°C. The time-temperature CAI relations (Fig. 6) have been investigated experimentally by Epstein et al. (1977) and Rejebian et al. (1987), and these data are used to constrain the time factor in the thermal history of the deposits.

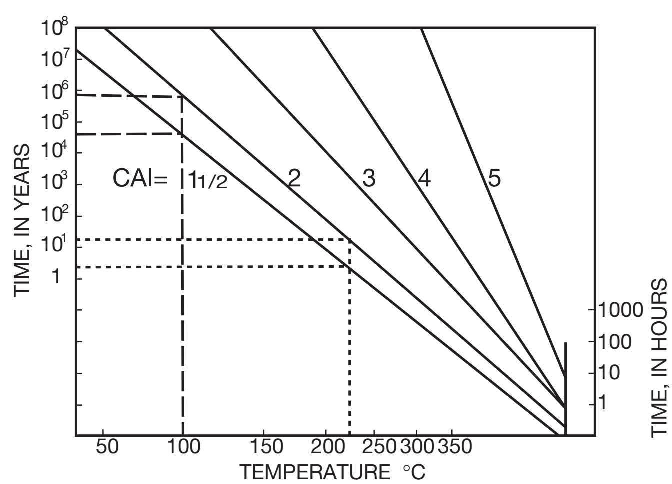


FIG. 6. A plot of the log of the reaction rate of experimentally derived conodont alteration as a function of heating time. Slanted lines numbered 1½ to 5 are conodont alteration index (CAI) values, vertical lines indicate temperature, and horizontal lines indicate time corresponding to Barneys Canyon data in Table 3. For example, conodonts heated to 225°C (vertical dotted line) for approximately two years would turn the color indicated by a CAI of 1½, whereas those heated for approximately 20 years would turn the color indicated by a CAI of 2. Modified slightly from Epstein et al. (1977).

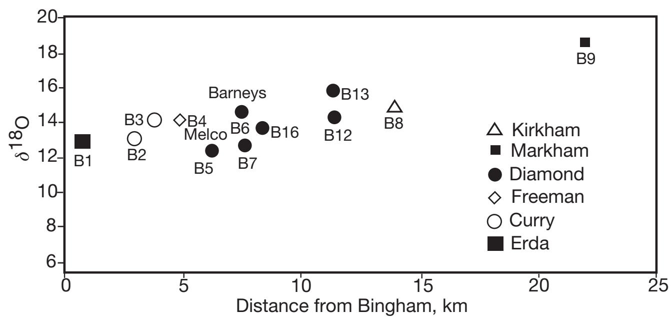


FIG. 7. Whole-rock $\delta^{18}O$ of quartzites (Table 5) versus distance north from the Bingham pit. Samples are along the axis of the Copperton anticline. Curry = Curry Peak Formation, Diamond = Diamond Creek Formation, Erda = Erda Formation, Freeman = Freeman Peak Formation, Kirkham = Kirkham Formation, and Markham = Markham Member of the Bingham Mine Formation.

*Organic indicators*

Bitumen appears to be formed from petroleum that was caught up or generated in the low-temperature hydrothermal system. During heating petroleum loses its volatiles, and ultimately it converts to solid bitumen that remains in the rock. The response time for the conversion of petroleum to bitumen by heating is rapid, which makes bitumen a sensitive indicator of maximum temperature conditions, since time is not a significant factor in recording the maximum temperature.

The limited bitumen reflectance data (Table 4) also indicate that these regional samples have not been heated above the oil window of about 150°C. A temperature indication of 220°C from vitrinite reflectance (Table 4, sample B6C) is not considered statistically valid because of insufficient data (Barker and Pawlewicz, 1993).

*Interpretation of integrated data*

The thermal data from zircon and apatite fission-track dating, CAI, and bitumen reflectance all show that the regional sedimentary rocks in the middle part of the northern Oquirrh Mountains, between the Bingham Canyon deposit and the Great Salt Lake, have not been regionally heated above about 140ºC since the rocks were formed.

A paleothermal anomaly related to the Bingham Canyon porphyry deposit extends at least 7.5 km to the north and includes both the Melco and Barneys Canyon gold deposits. It can be detected and mapped by a variety of thermally sensitive techniques. Figure 4 shows that apatite fission tracks were totally reset to about 37 Ma, the age of the Bingham porphyry Cu-Au-Mo deposit, all the way from the Bingham pit to Melco, a distance of 6 km, indicating that temperatures exceeded 100°C throughout this distance. The gold deposits are located on the periphery of the Bingham hydrologic system at approximately the 100°C isotherm and were not heated above 140°C for a sustained time based on the combined data of apatite fission track, CAI, and bitumen reflectance.

The maximum sustained temperature at the Melco deposit is constrained in three ways to between 100°C and 140°C: (1) a CAI of 2 (Table 3, sample B5A) for conodonts from a carbonate layer at Melco, which indicates maximum sustained heating to between 60° and140°C, (2) apatite fission tracks (Table 2, Figure 5, sample B5) that are totally annealed to the age of the Bingham intrusive complex, indicating temperatures of 100°C or higher, and (3) solid bitumen reflectance values of 0.95 percent, which indicate a temperature of about

TABLE 6. Whole-Rock Oxygen Isotope Data and Selected Elements in Samples from the Melco Traverse

| Sample | $\delta^{18}O$ (‰) | Au (ppb) | Au (oz/ton) | Ag (ppm) | Al (%) | As (ppm) | Ba (ppm) | Ca (%) | Cd (ppm) | Co (ppm) | Cr (ppm) | Cu (ppm) | Fe (%) | K (%) |
|---|---|---|---|---|---|---|---|---|---|---|---|---|---|---|
| B-17 | 15.7 | 10 | — | <0.2 | 0.06 | 10 | 10 | 1.58 | <0.5 | 1 | 54 | 7 | 0.21 | 0.01 |
| B-18 | 13.9 | 55 | — | <0.2 | 0.05 | 20 | 310 | 0.08 | <0.5 | <1 | 74 | 7 | 0.2 | 0.02 |
| B-20 | 12.6 | 320 | — | 0.4 | 0.21 | 326 | 1840 | 0.06 | 1.5 | 3 | 105 | 5 | 0.95 | 0.07 |
| B-21 | 11.7 | 85 | — | <0.2 | 0.4 | >10,000 | 3140 | 0.03 | <0.5 | 1 | 69 | 4 | 1.26 | 0.01 |
| B-22 | 6.4 | 30 | — | <0.2 | 0.56 | 444 | 210 | 0.07 | <0.5 | <1 | 28 | 3 | 0.26 | <.01 |
| B-19A | 12.9 | >10,000 | 0.363 | <0.2 | 0.16 | 442 | 80 | 0.08 | <0.5 | 16 | 54 | 11 | 1.62 | 0.06 |
| B-19 | 12.6 | 4,830 | — | <0.2 | 0.3 | 2,900 | 790 | 0.07 | 1 | <1 | 82 | 5 | 0.46 | 0.05 |
| B-23 | 12.4 | 10 | — | <0.2 | 0.11 | 56 | 40 | 0.03 | <0.5 | <1 | 51 | 2 | 0.1 | <.01 |
| B-24 | 12.8 | 5 | — | <0.2 | 0.15 | 112 | 500 | 0.06 | <0.5 | <1 | 98 | 9 | 0.42 | 0.02 |
| B-25 | 10.9 | 5 | — | <0.2 | 0.2 | 242 | 30 | 0.06 | <0.5 | 1 | 13 | 4 | 0.85 | <.01 |

| Sample | Mg (%) | Mn (ppm) | Mo (ppm) | Ni (ppm) | P (ppm) | Pb (ppm) | S (%) | Sb (ppm) | Sr (ppm) | Ti (%) | Tl (ppm) | V (ppm) | Zn (ppm) | Dist |
|---|---|---|---|---|---|---|---|---|---|---|---|---|---|---|
| B-17 | 0.04 | 125 | 3 | 5 | 70 | <2 | <.01 | <2 | 1 | <0.01 | <10 | 2 | 10 | 0 |
| B-18 | 0.01 | 5 | <1 | 13 | 70 | 6 | 0.01 | <2 | 4 | <0.01 | <10 | 1 | 10 | 29 |
| B-20 | 0.01 | 10 | 1 | 10 | 130 | 12 | 0.06 | <2 | 22 | <0.01 | <10 | 1 | 16 | 47 |
| B-21 | <0.01 | 5 | 11 | 3 | <10 | 10 | 0.04 | 12 | 11 | <0.01 | 140 | 4 | 28 | 61 |
| B-22 | <0.01 | <5 | <1 | 1 | 110 | 24 | 0.01 | <2 | 110 | <0.01 | <10 | 14 | 6 | 82 |
| B-19A | 0.01 | 25 | 9 | 30 | 40 | 14 | 1.63 | <2 | 10 | <0.01 | 10 | 4 | 6 | 85 |
| B-19 | 0.01 | 5 | 3 | 2 | 40 | 6 | <.01 | 10 | 9 | <0.01 | 260 | 3 | 4 | 87 |
| B-23 | <.01 | <5 | <1 | 1 | 40 | 4 | <.01 | <2 | 29 | <0.01 | <10 | 3 | 2 | 97 |
| B-24 | 0.1 | 5 | 1 | 4 | 10 | 8 | 0.17 | <2 | 8 | <0.01 | <10 | 1 | 2 | 123 |
| B-25 | <.01 | 15 | 3 | 9 | 60 | 6 | <.01 | <2 | 34 | <0.01 | <10 | 6 | 40 | 159 |

Acid digestion and ICP-AES analyses by ALS Chemex, Vancouver, BC; gold by fire assay
Dist = projected distance along a line between samples B17 and B25 in Figure 9

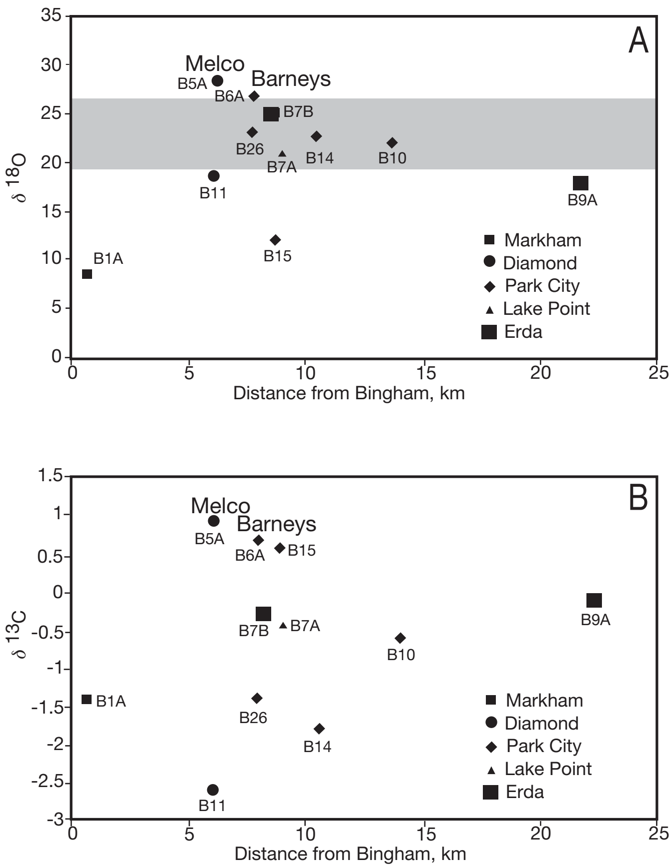


FIG. 8. A) Whole-rock $\delta^{18}O$ of limestone (Table 5) versus distance north from the Bingham pit. Gray band shows range of $\delta^{18}O$ values for unaltered Paleozoic sedimentary carbonate rocks in the Great Basin (Hofstra and Cline, 2000). Diamond = Diamond Creek Formation, Erda = Erda Formation, Lake Point = Lake Point Limestone, Markham = Markham Member of the Bingham Mine Formation, Park City = Park City Formation. B) $\delta^{13}C$ of limestone versus distance north from the Bingham pit.

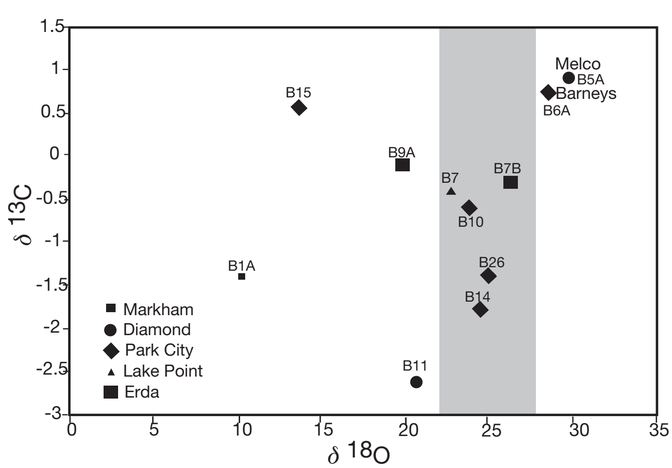


FIG. 9. $\delta^{13}C$ versus $\delta^{18}O$ of carbonate host rocks shown in Figure 8A and 8B. Symbols show different formations. Gray band shows range of $\delta^{18}O$ values for unaltered sedimentary carbonate rocks in the Great Basin (Hofstra and Cline, 2000). Diamond = Diamond Creek Formation, Erda = Erda Formation, Lake Point = Lake Point Limestone, Markham = Markham Member of the Bingham Mine Formation, Park City = Park City Formation.

100°C (Barker and Bone, 1995; Table 4, sample B5A). These independent thermal sensors indicate that maximum sustained temperatures were about 100°C within 3 to 7.5 km from the Bingham porphyry copper deposit.

The maximum sustained temperature at Barneys Canyon is constrained to about 100°C because (1) the fission tracks in zircon are not reset, which limits the temperature to less than 225°C to 250°C, (2) the fission tracks in apatite are partly reset, which limits the temperature to about 100°C, and (3) a CAI of 1.5 (Table 3, sample B6A), which indicates maximum sustained heating was about 90°C. This temperature is reasonable, because the Barneys Canyon deposit is about 1.5 km farther away from the Bingham deposit than the Melco deposit.

Conodonts are quite sensitive indicators of temperature and time. If the sustained temperature reached in the host rocks of Barneys Canyon was about 100°C (Fig. 6, vertical dashed line), the observed CAI of 1.5 indicates they were heated about 50,000 years. A CAI of 2 would correspond with a heating time of about$10^6$ yrs. Therefore, the conodont data, in conjunction with the other thermal indicators, are interpreted to constrain the hydrothermal system to between 50,000 and 1 m.y. duration.

The CAI of 2 at Melco, in agreement with the apatite data, indicates that the host rocks were heated to sustained temperatures between 100°C and 140°C, which indicates that it took $10^5$ to $10^6$ years to form. Higher temperatures result in a geologically unreasonably short amount of time for a significant ore deposit to form.

## Stable Isotopes

The whole rock stable isotope data on quartzite and limestone support the hypothesis that gold mineralization at Barneys Canyon and Melco formed by mixing of fluids within the distal part of the thermal anomaly related to the Bingham porphyry orebody. The evidence from the quartzite is less clear than the evidence from the limestone. Quartzite generally contains rounded quartz grains that locally display pressure solution effects and do not exhibit overgrowths. Quartzite also contains generally 5 to 10 percent of other detrital grains, mostly zircon, apatite, and feldspar, and clay minerals in the matrix, of which the clay is relatively reactive. At the temperatures considered in this study, isotopic exchange in quartzite most likely occurred in the reactive matrix material. Table 5 and Figure 7 show that the whole rock $\delta^{18}O$ values of the quartzite generally increase northward away from the Bingham pit from 12.5 per mil to as much as 18.6 per mil throughout a 22 km distance. These data show an approximate increase of $\delta^{18}O$ values by about 2 per mil within about 12 km of Bingham and an increase of nearly 6 per mil at the most distal sampling point. This overall trend is interpreted to reflect the widespread exchange of isotopically light meteoric water with the matrix minerals in the quartzite wall rocks, as has been documented around many intrusions and epigenetic ore deposits (Taylor, 1997; Hofstra and Rye, 1998). Variations in $\delta^{18}O$ of the quartzites exist within the trend, especially between 6 and 8 km; $\delta^{18}O$ values at Barneys Canyon (B6) are notably high and values at Melco (B5) are notably low. The scatter is interpreted to reflect variations in the amount of clay matrix and variable mixing of isotopically light water with largely fracture-controlled, isotopically heavy, presumably

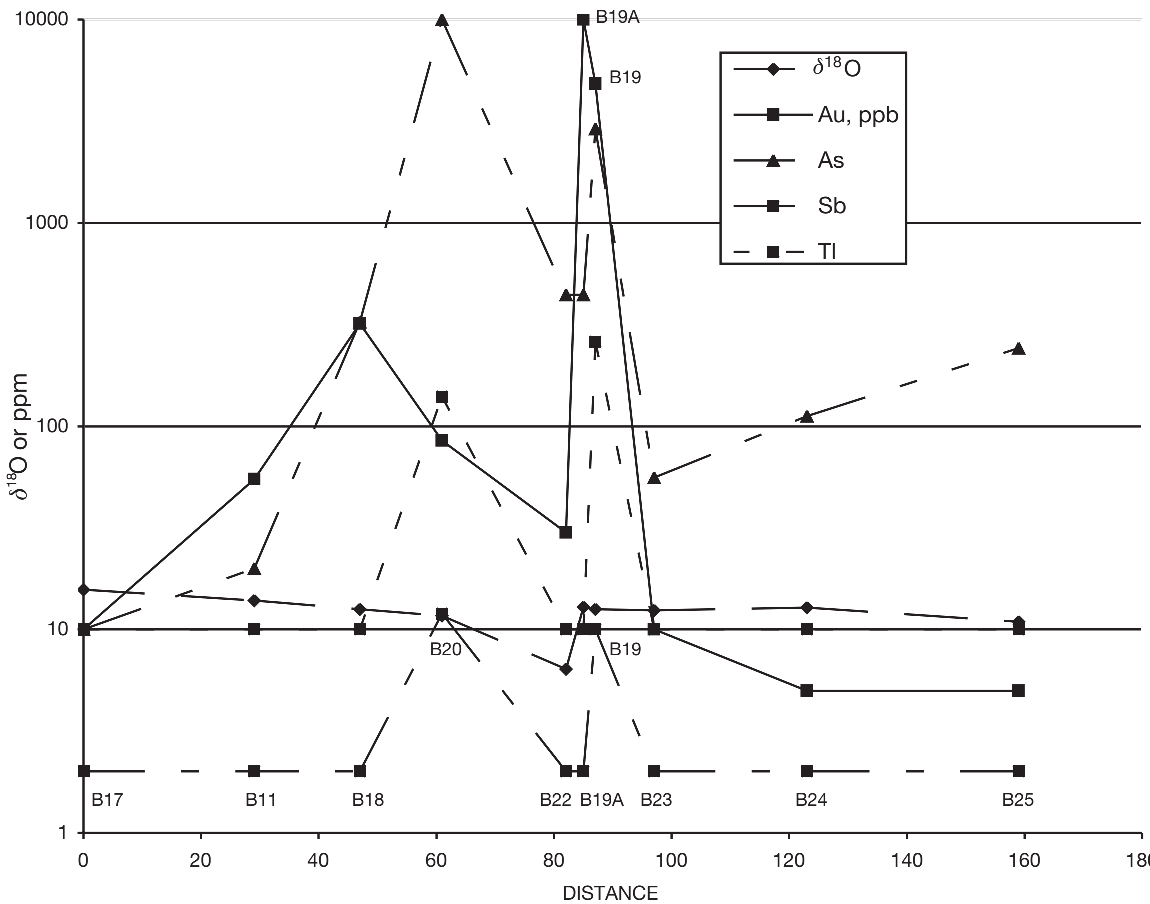


FIG. 10. Chemistry of quartzite samples from a traverse of the mineralized areas of the Melco gold deposit. Distance represents sample locality data projected to a line between B17 and B25 in Figure 3.

acidic water, as described further on. The variation in whole-rock $\delta^{18}O$ depends on the degree of mixing, proximity to fractures, amount of clay or carbonate in the matrix, and the temperature of the fluids involved.

Oxygen isotope ratios in a series of whole rock samples from approximately the same stratigraphic level in quartzite and across the orebody at Melco (Figs. 3 and 10) showed variations from 10.9 per mil to 15.7 per mil; one low $\delta^{18}O$ value was only 6.4 per mil (Fig. 10). Sample 22, which has the lowest $\delta^{18}O$, contains at least twice the amount of matrix clay as the other samples, contains significantly lower concentrations of Au, As, Sb, and Tl, and is closely related to a major fracture. These characteristics are interpreted to reflect exchange with fluids containing only isotopically light water and no component of isotopically heavy waters.

Oxygen and carbon isotope ratios of limestone were determined along the regional traverse (Table 5, Figs. 8A, B and 9). The oxygen and carbon isotope compositions of carbonate do not vary systematically with distance from the Bingham Canyon pit (Figs. 8A, B and 9). In general, hydrothermal fluids do not move through limestone as pervasively as they do through permeable quartzites (Pinckney and Rye, 1972; Rye et al., 1976). Isotopic exchange in carbonate rocks requires recrystallization of the carbonate; leaching or corrosion or partial dissolution of carbonate minerals without recrystallization does not result in isotopic exchange. The samples closest to Bingham have the lowest $\delta^{18}O$ values, whereas the Melco and Barneys Canyon samples have the highest $\delta^{18}O$ and highest $\delta^{13}C$ values. The values for most of the other samples, except for the one adjacent to the Bingham Canyon pit, fall in or adjacent to the range for unaltered Paleozoic limestone in the Great Basin (Hofstra and Cline, 2000). The Bingham sample (B1A) clearly reflects exchange with meteoric water (Fig. 8A). The Melco and Barneys Canyon samples have been recrystallized, and grain size increased from about 10 to 20 micrometers to about 75 to 100 micrometers and triple junctions developed where the grains meet. $\delta^{18}O$ values are consistent with exchange with isotopically heavy waters at low temperatures. For alteration at 100°C, the $\delta^{18}O$ values of nearly 30 per mil for the limestone at the Melco and Barneys Canyon deposits are consistent with equilibrium exchange with fluids having $\delta^{18}O_{H_2O}$ of 13 per mil.

*Possible sources of $^{18}O$ enrichment*

Isotopically heavy waters such as noted here are distinctive and their association with the disseminated gold deposit is likely not fortuitous. Such waters may have formed on the surface of the Bingham stratovolcano, for example in a crater lake or around fumaroles. These waters were likely acidic because of the oxidation of sulfur-bearing gases and release of HCl from the magma, and they likely had high $\delta^{18}O$ values owing to evaporation at elevated temperatures (e.g., Rowe, 1994; Varekamp, 2002, Rye, 2004; Zimbelman et al., 2004). Such oxidizing, acidic waters are common in the crater lakes of active volcanoes. Field studies and Landsat imagery of active volcanoes also have shown that such acidic fluids can drain back through permeable layers parallel to the slopes of the volcano beneath the surface lava flows (e.g., Rowe, 1994). This alteration removes the pH buffering capacity of the rocks and aids the downward penetration of fluids. An excellent example of the distribution of acid-altered rocks in a stratovolcano can be seen in the Thematic Mapper image shown in Figure 11. This is possibly what the area of Bingham Canyon, Barneys Canyon, and Melco looked like 37 m.y. ago with the porphyry forming beneath the center of the volcano and the gold deposits under the flanks.

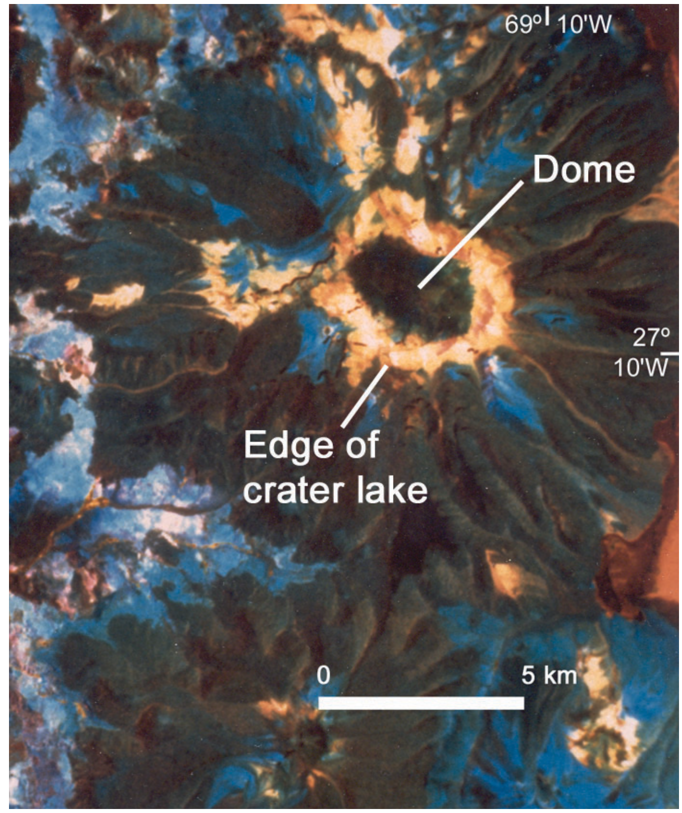


FIG. 11. Thematic Mapper image of the Miocene Maricunga volcano in northern Chile. The image shows what the Bingham Canyon–Barneys Canyon–Melco area may have looked like 37 m.y. ago. The dark, relatively fresh, radially outward-dipping lava flows on the surface of the volcano can be readily seen. Yellow reveals the distribution of rocks altered to alunite and kaolinite. The yellow circular feature consists of advanced argillic-altered sediments at the edge of the crater lake, the center of which was intruded by an unaltered dome. The yellow stripes on the volcano flanks mark areas where landslides and sector collapse have occurred, revealing the altered rocks beneath the surface flows. The isolated yellow spots near the base of the volcano mark locations where acidic hot springs emanated. Image courtesy of Lawrence C. Rowan and Barbara A. Eiswerth. Source, unpublished U.S. Geological Survey files.

## Discussion and Conclusions

### *Fluid inclusions*

The thermal data reported here are significantly different from the reported fluid inclusion homogenization temperatures from quartz and barite at the Barneys Canyon deposit (Presnell and Parry, 1996). Presnell and Parry reported homogenization temperatures that range from 130° to 393°C for 53 inclusions in six quartz samples and 10 inclusions in two barite samples. The data are scattered throughout this range but show weak modes at 225°C and 345°C. The barite data overlap the quartz data in the range 260°C to 390°C. Corresponding salinities are mostly 0 to 3 wt percent equivalent NaCl. These results may reflect rare instances of channeled flow as described previously, as silicification of any kind is unusually rare, and discrete quartz veins, whether related to gold mineralization or otherwise, are scarce to absent. Also, barite can be unreliable as a fluid inclusion host mineral especially at temperatures above 250°C (Ulrich and Bodnar, 1988). Most other evidence does not support the high temperatures indicated by the fluid inclusion homogenization results. The alteration mineral kaolinite (stable at <270°C) is present rather than pyrophyllite, and marcasite and arsenic sulfides suggest temperatures lower than 250°C (Murochick, 1992). Conodont alteration indices, fission tracks, and vitrinite reflectance also indicate lower temperatures than reported by Presnell and Parry (1996).

It is difficult to unequivocally date the gold deposits because any minerals or event that can be dated by current methodologies is subject to alternative interpretations based on the relationship of mineralization to the mineral or event dated. We think the most plausible interpretation is one that considers and integrates the thermal history, spatial relationship of mineralization to illite, chemical zoning of the hydrothermal system, genetic implications of heavy oxygen and carbon isotopes, and hydrologic limitations in the formulation of a model. The lack of anhydrite in the Bingham porphyry deposit coupled with the narrow range of $\delta^{34}S$ values for sulfides (Field, 1966) most likely reflects the reduced nature of the main stage fluids. We conclude that the Barneys Canyon and Melco gold deposits, the nearby satellite deposits, and perhaps the proximal occurrences such as Main Hill that developed in late structures cutting the Bingham porphyry likely formed during the time that the reduced, gold-bearing fluids that deposited the bulk of the Bingham copper mineralization cooled and mixed with surficial, oxidized, acidic fluids within the collapsing system as shown schematically in Figure 12. Mixing of late-stage, gold-bearing, reduced fluids with isotopically heavy, K-rich, acidic fluids may have caused the deposition of the gold under illite-stable conditions. The observation by Presnell and Parry (1992) that the orebody at Barneys Canyon is associated with illite rather than kaolinite may reflect a high potassium content in the acidic fluids and strengthens the case for a mixing model. The presence of marcasite might also reflect deposition by mixing with an acidic solution at temperatures <250°C (Murowchick, 1992; Vaughan and Craig, 1997). Barite is present in both massive form and as crystals along faults and fractures at Melco, and at Barneys Canyon, barite was the host mineral for some of the analyzed fluid inclusions (Presnell, 1992). The barite may

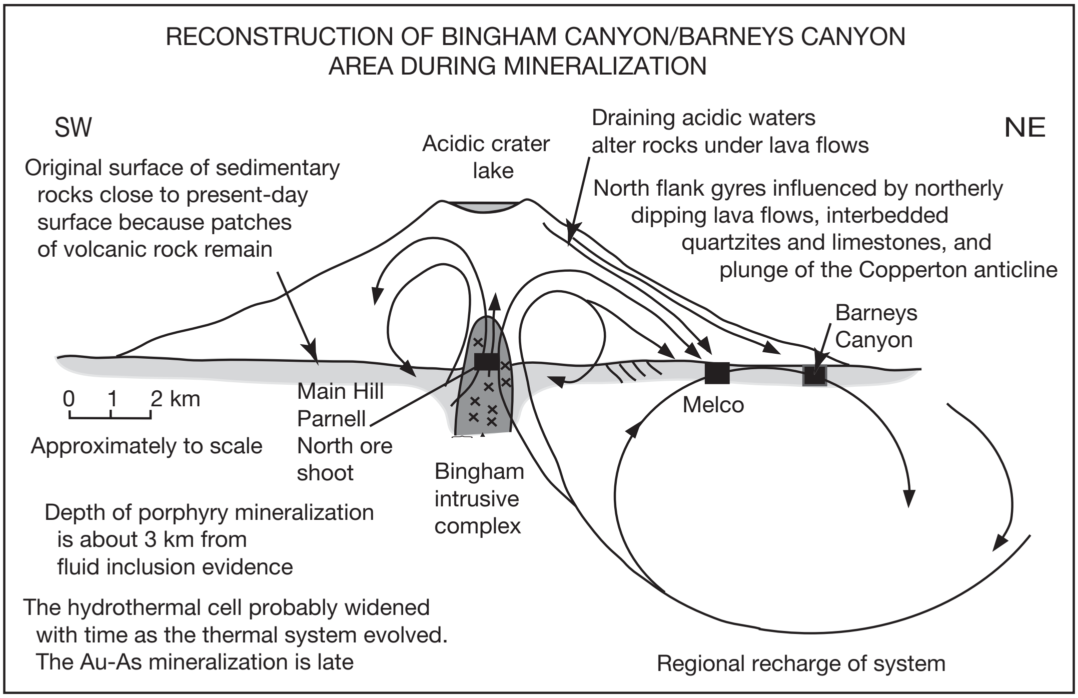


FIG. 12. Schematic hydrologic model of the formation of late stage disseminated gold deposits associated with the Bingham Canyon porphyry Cu-Au-Mo deposit.

reflect mixing of acidic, sulfate-rich fluids with barium-bearing fluids. The notable paucity of quartz associated with the gold argues against temperature decrease alone being a major factor in the localization of the gold. Fluid mixing likely occurred at the hydrologic juncture of the sedimentary rocks and overlying volcanic rocks, where the deposits are located (Fig. 12). The collapsing hydrothermal system decreased in size until it was confined to Bingham Canyon or may have become localized in late north-striking structures.

Sawkins (1984), Sillitoe (1988), Sillitoe and Bonham (1990), and other authors have proposed a genetic link between gold-rich porphyry systems and sedimentary rock-hosted, disseminated gold deposits. Babcock et al. (1995) proposed such a genetic link between the Bingham Canyon porphyry deposit and the Barneys Canyon and Melco gold deposits, but the evidence was equivocal (e.g., Presnell and Parry, 1996). This study presents new fission track, conodont CAI, solid bitumen reflectance, and stable isotope data that show that the hydrothermal system associated with the 37 Ma Bingham Canyon porphyry system extended far enough to encompass the gold deposits leaving behind a record of the paleothermal anomaly in the country rocks. The Melco and Barneys Canyon deposits most likely were formed at sustained temperatures of less than 140°C and close to the Bingham Canyon porphyry system 120°C isotherm.

The $\delta^{18}O$ values of quartzite, sampled along the axis of an anticline that was in place during mineralization, increase away from Bingham Canyon. Because the quartz grains in the quartzites are resistant to isotopic exchange and because, except locally, the clay matrix of the quartzite makes up no more than 15 percent of the total rock, a huge water-dominated system in permeable quartzite during the main stage Bingham Canyon mineralization is required to account for the isotopic shift. The regionally distributed carbonate rocks do not show systematic variation in their isotopic composition away from Bingham Canyon porphyry, which is consistent with observations reported elsewhere that isotopic exchange in carbonate rocks typically only occurs close to fractures. Hydrothermally altered and recrystallized limestone near fractures in the vicinity of the Melco and Barneys Canyon gold deposits are exceptionally enriched in $^{18}O$. These high $\delta^{18}O$ values require low temperature exchange with isotopically heavy fluids such as form on the surface of stratovolcanoes in crater lakes.

It is proposed that the gold was part of the late-stage, reduced Au-As mineralization that has been documented in the Bingham dispersal halo. In this model, isotopically heavy, acidic, sulfate-rich water that was draining downslope mixed with the reduced, $H_2S$-rich and Au-bearing, meteoric water at progressively deeper levels in a collapsing Bingham system. Deposition occurred dominantly by mixing, probably along a hydrologic interface near the sedimentary rock-volcanic rock contact. If this scenario is correct, all disseminated gold deposits that occur in late fractures in the area probably developed during the waning stages of the Bingham mineralizing system.

## Acknowledgments

We appreciate the thoughtful discussions, reviews, and advice we have had from many of our colleagues, especially Paul B. Barton, Jr., William L. Gunter, Mark Hannington, Anita G. Harris, Daniel O. Hayba, Albert H. Hofstra, David A. John, Stephen G. Peters, Ricardo D. Presnell, Ted G. Theodore, and an anonymous reviewer. We also appreciate Kennecott Corporation's help and cooperation in this study. David Sutphin and Jill Moebus helped draft the figures. Lawrence C. Rowan and Barbara A. Eisworth kindly contributed the Thematic Mapper image.

*January 6, 2003; January 19, 2004*

## REFERENCES

Arehart, G.B., Chakurian, A.M., Tretbar, D.R., Christensen, J.N., McInnes, B.A., and Donelick, R.A., 2003, Evaluation of radiometric dating of Carlin-type deposits in the Great Basin, western North America, and implications for deposit genesis: ECONOMIC GEOLOGY, v. 73, p. 235–248.

Armstrong, A.K., Theodore, T.G., Kotlyar, B.B., Lauha, E.G., Griffin, G.L., Lorge, D.L., and Abbott, E.W., 1997, Preliminary facies analysis of Devonian autochthonous rocks that host Au along the Carlin trend, Nevada, *in* Vikre, Peter, Thompson, T.B., Bettles, K., Christensen, Odin, and Parratt, R., eds., Carlin-Type Au Deposits Field Conference: Society of Economic Geologists Guidebook 28, p. 53–74.

Armstrong, A.K., Theodore, T.G., Oscarson, R.L., Kotlyar, B.B., Harris, A.G., Bettles, K.H., Lauha, E.A., Hipsley, R.A., Griffin, G.L., Abbott, E.W., and Cluer, J.K., 1998, Preliminary facies analysis of Silurian and Devonian autochthonous rocks that host gold along the Carlin trend, Nevada, *in* Tosdal, R.M., ed., Contributions to the Au metallogeny of the northern Great Basin: U.S. Geological Survey Open-File Report 98-338, p. 38–68.

Armstrong, R.L., 1968, Sevier orogenic belt in Nevada and Utah: Geological Society of America Bulletin, v. 79, p. 429–458.

Atkinson, W.W., and Einaudi, M.T., 1978, Skarn formation and mineralization in the contact aureole at Carr Fork, Bingham, Utah: ECONOMIC GEOLOGY, v. 73, p. 1326–1365.

Austin, G.W., and Gunter, W.L., 1997, Day three road log: Field trip to the Barneys Canyon and Melco mines, Utah, *in* John, D.A., and Ballantyne, G.H., eds., Geology and ore deposits of the Oquirrh and Wasatch Mountains, Utah: Society of Economic Geologists Guidebook 29, p. 255–256.

Babcock, R.C., Jr., Ballantyne, G.H., and Phillips, C.H., 1995, Summary of the geology of the Bingham district, Utah, *in* Pierce, F.W., and Bolm, J.G., eds., Porphyry copper deposits of the American Cordillera: Tucson, Arizona, The Arizona Geological Society Digest, v. 20, p. 316–335.

Ballantyne, G.H., 1998a, The Bingham district—product of a giant hydrothermal cell about a large gold-rich porphyry copper deposit [abs.]: Geological Society of Australia, 14th Australian Geological Convention, Townsville, Queensland, July 1998, p. 18.

——1998b, Sediment-hosted gold deposits in the Bingham district, Utah [abs.]: Geological Society of Nevada Newsletter, v. 12, no. 5.

Ballantyne, G.H., Smith, T.W., and Redmond, P.B., 1997, Distribution and mineralogy of gold and silver in the Bingham Canyon porphyry copper deposit, Utah, *in* John, D.A., and Ballantyne, G.H., eds., Geology and ore deposits of the Oquirrh and Wasatch Mountains, Utah: Society of Economic Geologists Guidebook 29, p. 47–153.

Barker, C.E., and Bone, Y., 1995, The minimal response to contact metamorphism by the Devonian Buchan Limestone, Buchan rift, Victoria, Australia: Organic Geochemistry, v. 22, no. 1, p. 151–164.

Barker, C.E., and Pawlewicz, M.J., 1993, An empirical determination of the minimum number of measurements needed to estimate the mean random vitrinite reflectance of disseminated organic matter: Organic Geochemistry, v. 20, no. 6, p. 643–651.

——1994, Calculation of vitrinite reflectance from thermal histories and peak temperature—A comparison of methods: "Reevaluation of vitrinite reflectance as a maturity parameter": American Chemical Society Symposium Series 570, p. 216–229.

Beaty, D.W., Cunningham, C.G., Harrison, W.J., Landis, G.P., Merchant, J.S., Naeser, C.W., and Wendlandt, R.F., 1990, Origin of the ore deposits at Gilmin, Colorado—Part VI. Discussion and development of a genetic mode, *in* Beaty, D.W., Landis, G.P., and Thompson, T.B., eds., Carbonate-hosted sulfide deposits of the central Colorado mineral belt: ECONOMIC GEOLOGY MONOGRAPH 7, p. 255–265.

Biek, R.F., Hylland, M.D., Welsh, J.E., and Lowe, Mike, 2000, Interim geologic map of the Center Creek Quadrangle, Wasatch County, Utah: Utah Geological Survey Open-File Report 370, 103 p.

Bowman, J.R., Parry, W.T., Kropp, W.P., and Kruer, S.A., 1987, Chemical and isotopic evolution of hydrothermal solutions at Bingham, Utah: ECONOMIC GEOLOGY, v. 82, p. 395–428.

Brandon, M.T., Roden-Tice, M.K., and Garver, J.L., 1998, Late Cenozoic exhumation of the Cascadia accretionary wedge in the Olympic Mountains, northwest Washington State: Geological Society of America Bulletin, v. 110, no. 8, p. 985–1009.

Cameron, D.E., and Garmoe, W.J., 1987, Geology of skarn and high-grade gold in the Carr Fork mine, Utah: ECONOMIC GEOLOGY, v. 82, p. 1319–1333.

Cathles, L.M., 1977, An analysis of the cooling of intrusives by groundwater convection which includes boiling: ECONOMIC GEOLOGY, v. 72, p. 804–826.

Chesley, J.T., and Ruiz, Joaquin, 1997, Preliminary Re-Os dating on molybdenite mineralization from the Bingham Canyon porphyry copper deposit, Utah, *in* John, D.A., and Ballantyne, G.H., eds., Geology and ore deposits of the Oquirrh and Wasatch Mountains, Utah: Society of Economic Geologists Guidebook 29, p. 165–169.

Cox, D.P., and Singer, D.A., eds., 1986, Mineral deposit models: U.S. Geological Survey Bulletin 1693, 379 p.

——1990, Descriptive and grade-tonnage models for distal-disseminated Ag-Au deposits: A supplement to U.S. Geological Survey Bulletin 1693: U.S. Geological Survey Open-File Report 90-282, 7 p.

——1992, Grade and tonnage model of distal disseminated Ag-Au, *in* Bliss, J.D., ed., Developments in mineral deposit modeling: U.S. Geological Survey Bulletin 2004, p. 20–22.

Cunningham, C.G., and Barton, P.B., Jr., 1984, Recognition and use of paleothermal anomalies as a new exploration tool [abs.]: Geological Society of America Abstracts with Programs, v. 16, no. 6, p. 481.

Cunningham, C.G., Naeser, C.W., Cameron, D.E., Barrett, L.F., Wilson, J.C., and Larson, P.B., 1987, The Pliocene paleothermal anomaly at Rico, Colorado, is related to a major molybdenum deposit [abs.]: Geological Society of America Abstracts with Programs, v. 19, no. 5, p. 268–269.

Deino, A., and Keith, J.D., 1997, Ages of volcanic and intrusive rocks in the Bingham mining district, Utah, *in* John, D.A., and Ballantyne, G.H., eds., Geology and ore deposits of the Oquirrh and Wasatch Mountains, Utah: Society of Economic Geologists Guidebook 29, p. 91–100.

Epstein, A.G., Epstein, J.B., and Harris, L.D., 1977, Conodont color alteration—An index to organic metamorphism: U.S. Geological Survey Professional Paper 995, 27 p.

Field, C.W., 1966, Sulfur isotope abundance data, Bingham District, Utah: ECONOMIC GEOLOGY, v. 61, p. 850–871

Galbraith, R.F., 1981, On statistical models for fission track counts, reply: Mathematical Geology, v. 13, p. 471–488.

Green, P.F., Duddy, I.R., Gleadow, A.J.W., and Lovering, J.F., 1989, Apatite fission-track analysis as a paleotemperatuure indicator for hydrocarbon exploration, *in* Naeser, N.D., and McCulloh, T.H., eds., Thermal history of sedimentary basins—Methods and case histories: New York, Springer-Verlag, p. 181–195.

Gunter, W.L., 1992, Geology of the Barneys Canyon gold deposit, Salt Lake County, Utah, *in* Wilson, J.R., ed., Field guide to geologic excursions in Utah and adjacent areas of Nevada, Idaho, and Wyoming: Utah Geological Survey Miscellaneous Publication 92-3, p. 307–311.

Gunter, W.L., and Austin, G.W., 1997, Geology of the Melco gold deposit, Oquirrh Mountains, Utah, *in* John, D.A., and Ballantyne, G.H., eds., Geology and ore deposits of the Oquirrh and Wasatch Mountains, Utah: Society of Economic Geologists Guidebook 29, p. 227–240.

Gunter, W.L., Hammitt, J.W., Babcock, R.C., Gibson, T.R., and Presnell, R.D., 1990, Geology of the Barneys Canyon and Melco gold deposits, Salt Lake County, Utah, *in* Hausen, D.M., ed., Gold '90: New York, American Institute of Mining Engineers, p. 41–59.

Harris, A.G., Wardlaw, B.R., Rust, C.C., and Merrill, G.K., 1980, Maps for assessing thermal maturity (conodont color alteration index maps) in Ordovician through Triassic rocks in Nevada and Utah and adjacent parts of Idaho and California: U.S. Geological Survey Miscellaneous Investigations Map I-1249, scale 1:2,500,000.

Hofstra, A.H., and Cline, J.S., 2000, Characteristics and models for Carlin-type deposits, *in* Hagemann, S.G., and Brown, P.E., eds., Gold in 2000: Reviews in Economic Geology, v. 13, p. 163–220.

Hofstra, A.H., and Rye, R.O., 1998, ?D and ?$^{18}$O data from Carlin-type Au deposits—Implications for genetic models, *in* Tosdal, R.M., ed., Contributions to the Au Metallogeny of northern Nevada: U.S. Geological Survey Open-File Report 98-338, p. 202–210.

Hofstra, A.H., Snee, L.W., Rye, R.O., Folger, H.W., Phinisey, J.D., Loranger, R.J., Dahl, A.R., Naeser, C.W., Stein, H.J., and Lewchuk, M., 1999, Age constraints on Jerritt Canyon and other Carlin-type gold deposits in the western United States—Relationship to min-Tertiary extension and magmatism: ECONOMIC GEOLOGY, v. 94, p. 769–802.

Hofstra, A.H., John, D.A., and Theodore, T.G., eds., 2003, A special issue devoted to gold deposits in northern Nevada—Part 2. Carlin-type deposits: ECONOMIC GEOLOGY, v. 98, p. 1063–1252.

Hurford, A.J., 1986, Cooling and uplift patterns in the Lepointine Alps, south central Switzerland, and an age on vertical movement on the Insubric fault line: Contributions to Mineralogy and Petrology, v. 92, p. 413–427.

Hurford, A.J., and Green, P.F., 1983, The zeta age calibration of fission-track dating: Isotope Geoscience, v. 1, p. 285–317.

Hunt, J.M., 1995, Petroleum geochemistry and geology—second edition: San Francisco, W.H. Freeman, 743 p.

James, A.H., Smith, W.H., and Welsh, J.E., 1961, General geology and structure of the Bingham mining district, Utah: Utah Geological Society Guidebook 16, p. 101–119.

John, D.A., and Ballantyne, G.H., eds., 1997, Geology and ore deposits of the Oquirrh and Wasatch Mountains, Utah: Society of Economic Geologists Guidebook 29, 256 p.

John, E.C., 1978, Mineral zones in the Utah Copper orebody: ECONOMIC GEOLOGY, v. 73, p. 1250–1259.

Kendrick, M.A., Burgess, R., Pattrick, R.A.D., and Turner, G., 2001, Halogen and Ar-Ar age determinations of inclusions within quartz veins from porphyry copper deposits using complementary noble gas extraction techniques: Chemical Geology, v. 177, p. 351–370.

Krahulec, K.A., 1997, History and production of the West Mountain (Bingham) mining district, Utah, *in* John, D.A., and Ballantyne, G.H., eds., Geology and ore deposits of the Oquirrh and Wasatch Mountains, Utah: Society of Economic Geologists Guidebook 29, p. 189–217.

Laes, D.Y.M., Krahulec, K.A., and Ballantyne, G.H., Compilers, 1997, Geologic map of the Oquirrh Mountains, Utah, *in* John, D.A., and Ballantyne, G.H., eds., Geology and ore deposits of the Oquirrh and Wasatch Mountains, Utah: Society of Economic Geologists Guidebook 29, scale 1:62,500.

Lanier, G., John, E.C., Swensen, A.J., Reid, J.E., Bard, C.E., Caddey, S.W., and Wilson, J.C., 1978a, General geology of the Bingham mine, Bingham Canyon, Utah: ECONOMIC GEOLOGY, v. 73, p. 1228–1241.

Lanier, G., Raab, W.J., Folsom, R.B., and Cone, S., 1978b, Alteration of equigranular monzonite, Bingham mining district, Utah: ECONOMIC GEOLOGY, v. 73, p. 1270–1286.

Larson, P.B., Cunningham, C.G., and Naeser, C.W., 1994, Large-scale alteration effects in the Rico paleothermal anomaly, southwest Colorado: ECONOMIC GEOLOGY, v. 89, p. 1769–1779.

Miller, D.M., 1990, Mesozoic and Cenozoic tectonic evolution of the northeastern Great Basin, *in* Shaddrick, D.R., Kizis, J.A., and Hunsaker, E.L., eds., Geology and ore deposits of the northeastern Great Basin: Geological Society of Nevada and U.S. Geological Survey Field Trip 5 Guidebook, p. 43–73.

Murowchick, J.B., 1992, Marcasite inversion and petrographic determination of pyrite ancestry: ECONOMIC GEOLOGY, v. 87, p. 1141–1152.

Naeser, C.W., 1979, Fission-track dating and geologic annealing of fission tracks, *in* Jager, E., and Hunziker, J.C., Lectures in isotope geology: Berlin, Springer-Verlag, p. 154–169.

——1981, The fading of fission tracks in the geologic environment—Data from deep drill holes: Nuclear Tracks, v. 5, p. 248–250.

Naeser, C.W., Cunningham, C.G., Marvin, R.F., and Obradovich, J.D., 1980, Pliocene intrusive rocks and mineralization near Rico, Colorado: ECONOMIC GEOLOGY, v. 75, p. 122–127.

Norton, D.L., 1978, Sourcelines, source regions, and pathlines for fluids in hydrothermal systems related to cooling plutons: ECONOMIC GEOLOGY, v. 73, p. 21–28.

Parry, W.T., Wilson, P.N., Jasumback, M.D., and Heizler, M.T., 1997, Clay mineralogy and $^{40}Ar/^{39}Ar$ dating of phyllic and argillic alteration at Bingham Canyon, Utah, *in* John, D.A., and Ballantyne, G.H., eds., Geology and ore deposits of the Oquirrh and Wasatch Mountains, Utah: Society of Economic Geologists Guidebook 29, p. 171–188.

Parry, W.T., Wilson, P.N., Moser, D., and Heizler, M.T., 2001, U-Pb dating of zircon and $^{40}Ar/^{39}Ar$ dating of biotite at Bingham, Utah: ECONOMIC GEOLOGY, v. 96, p. 1671–1683.

Peters, S.G., Mihalasky, M.J., and Theodore, T.G., 2004, Assessment for sedimentary-rock hosted Au-Ag deposits, Chapter 8, *in* Wallace, A.R., Ludington, Steve, Mihalasky, M.J., Peters, S.G., Ponce, D.A., Theodore, T.G, John, D.A., and Berger, B.R, Assessment of undiscovered metallic mineral resources, Humboldt River basin, northern Nevada: U.S. Geological Survey Bulletin B-2218, in press.

Peters, W.C., James, A.H., and Field, C.W., 1966, Geology of the Bingham Canyon porphyry copper deposit, Utah, *in* Titley, S.R., and Hicks, C.L., eds., Geology of the porphyry copper deposits, southwestern North America: Tucson, Arizona, The University of Arizona Press, p. 165–175.

Phillips, C.H., Smith, T.W., and Harrison, E.D., 1997, Alteration, metal zoning, and ore controls in the Bingham Canyon porphyry copper deposit, Utah, *in* John, D.A., and Ballantyne, G.H., eds., Geology and ore deposits of the Oquirrh and Wasatch Mountains, Utah: Society of Economic Geologists Guidebook 29, p. 171–188.

Pinckney, D.M., and Rye, R.O., 1972, Variation of $O^{18}/O^{16}$, $C^{13}/C^{12}$, texture and mineralogy in altered limestone in the Hill mine, Cave-in-Rock district, Illinois: ECONOMIC GEOLOGY, v. 67, p. 1–18.

Presnell, R.D., 1992, Geology and geochemistry of the Barneys Canyon gold deposit, Salt Lake County, Utah: Unpublished Ph.D. dissertation, Salt Lake City, University of Utah, 363 p.

——1997, Structural controls on the plutonism and metallogeny in the Wasatch and Oquirrh Mountains, Utah, *in* John, D.A., and Ballantyne, G.H., eds., Geology and ore deposits of the Oquirrh and Wasatch Mountains, Utah: Society of Economic Geologists Guidebook 29, p. 1–9.

Presnell, R.D., and Parry, W.T., 1992, Argillic alteration at the Barneys Canyon gold deposit: Field guide to geologic excursions in Utah and adjacent areas of Nevada, Idaho, and Wyoming: Utah Geological Survey Miscellaneous Publication 92-3, p. 313–318.

——1995, Evidence of Jurassic tectonism from the Barneys Canyon gold deposit, Oquirrh Mountains, Utah, *in* Miller, D.M., and Busby, C., Jurassic magmatism and tectonics of the North American Cordillera: Geological Society of America Special Paper 299, p. 313–326.

——1996, Geology and geochemistry of the Barneys Canyon gold deposit, Utah: ECONOMIC GEOLOGY, v. 91, p. 273–288.

Rejebian, V.A., Harris, A.G., and Huebner, J.S., 1987, Conodont color and textural alteration: An index to regional metamorphism, contact metamorphism, and hydrothermal alteration: Geological Society of America Bulletin, v. 99, p. 471–479.

Rose, A.W., 1970, Zonal relations of wallrock alteration and sulfide distribution at porphyry copper deposits: ECONOMIC GEOLOGY, v. 65, p. 920–936.

Rowe, G.L., Jr., 1994, Oxygen, hydrogen, and sulfur isotope systematics of the crater lake system of Poas volcano, Costa Rica: Journal of volcanology and geothermal research, v. 28, p. 263–287.

Rubright, R.D., and Hart, O.J., 1968, Non-porphyry ores of the Bingham district, Utah, *in* J.D. Ridge, ed., Ore deposits in the United States 1933–1967: American Institute of Mining, Metallurgical and Petroleum Engineers, v. 1, p. 966–991.

Rye, R.O., 2004, A review of the stable-isotope geochemistry of sulfate minerals in selected igneous environments and related hydrothermal systems: Chemical Geology, in press.

Rye, R.O., Schuiling, R.D., Rye, D.M., and Jansen, J.B.H., 1976, Carbon, hydrogen and oxygen isotope studies of the regional metamorphic complex at Naxos, Greece: Geochimica et Cosmochimica Acta, v. 40, p. 1031–1049.

Sawkins, F.J., 1984, Metal deposits in relation to plate tectonics: New York, Springer Verlag, 325 p.

Sillitoe, R.H., 1988, Gold and silver deposits in porphyry systems, *in* Schafer, R.W., Gooper, J.J., and Vikre, P.G., eds., Bulk mineable precious metal deposits of the western United States: Geological Society of Nevada Symposium Proceedings, p. 233–257.

Sillitoe, R.H., and Bonham, H.F., Jr., 1990, Sediment-hosted gold deposits: Distal products of magmatic-hydrothermal systems: Geology, v. 18, p. 157–161.

Snoke, A.W., and Miller, D.M., 1988, Metamorphic and tectonic history of the northeastern Great Basin, *in* Ernst, W.G., ed., Metamorphism and crustal evolution of the western United States: p. 606–648.

Taylor, H.P., Jr., 1997, Oxygen and hydrogen isotope relationships in hydrothermal mineral deposits, *in* Barnes, H.L., ed., Geochemistry of hydrothermal ore deposits—third edition: New York, John Wiley, p. 229–302.

Theodore, T.G., 2000, Geology of pluton-related gold mineralization at Battle Mountain, Nevada: University of Arizona and U.S. Geological Survey Center for Mineral Resources Monograph 2, 271 p.

Thorman, C.H., Ketner, K.B., and Peterson, Fred, 1992, The Middle to Late Jurassic Elko orogeny in eastern Nevada and western Utah [abs.]: Geological Society of America Abstracts with Programs, v. 24, no. 6, p. 66.

Ulrich, M.R., and Bodnar, R.J., 1988, Systematics of stretching of fluid inclusions II: Barite at 1 atm confining pressure: ECONOMIC GEOLOGY, v. 83, p. 1037–1046.

Varekamp, J.C., 2002, An active magmatic hydrothermal system at Copahue volcano [abs.]: V.M. Goldschmidt Conference, 12th, Davos, Switzerland, 2002, Geochimica et Cosmochimica Acta supplement, v. 66, no. 15A, p. A800.

Vaughan, D.J., and Craig, J.R., 1997, Sulfide ore mineral stabilities, morphologies, and intergrowth textures, *in* Barnes, H.L., ed., Geochemistry of hydrothermal ore deposits—third edition: New York, John Wiley, p. 367–434.

Waite, K.A., Keith, J.D., Christiansen, E.H., Whitney, J.A., Hattori, Keiko, Tingey, D.G., and Hook, C.J., 1997, Petrogenesis of the volcanic and intrusive rocks associated with the Bingham Canyon porphyry Cu-Au-Mo deposit, Utah, *in* John, D.A., and Ballantyne, G.H., eds., Geology and ore deposits of the Oquirrh and Wasatch Mountains, Utah: Society of Economic Geologists Guidebook 29, p. 69–100.

Warnaars, F.W., Smith, W.H., Bray, R.E., Lanier, G., and Shafiqullah, M., 1978, Geochronology of igneous intrusions and porphyry copper mineralization at Bingham, Utah: ECONOMIC GEOLOGY, v. 73, p. 1242–1249.

Zimbelman, D.R., Rye, R.O., and Breit, G.N., 2004, Origin of sulfate minerals in active andesitic stratovolcanoes: Chemical Geology, in press.